NUMERICAL METHODOLOGY FOR FEASIBILITY ANALYSIS
OF GROUND SOURCE HEAT PUMPS

A THESIS SUBMITTED TO
THE BOARD OF CAMPUS GRADUATE PROGRAMS
OF MIDDLE EAST TECHNICAL UNIVERSITY
NORTHERN CYPRUS CAMPUS

BY

KUMUDU JANANI GAMAGE

IN PARTIAL FULLFILLMENT OF THE REQUIREMENTS
FOR
THE DEGREE OF MASTER OF SCIENCE
IN
SUSTAINABLE ENVIRONMENT AND ENERGY SYSTEMS

AUGUST 2014

Approval of the Board of Graduate Programs

_____

Prof. Dr. Tanju Mehmetoğlu
Chair person

I certify that this thesis satisfies all the requirements as a thesis for the degree of Master of Science.

_____

Assoc. Prof. Dr. Ali Muhtaroğlu
Program Coordinator

This is to certify that we have read this thesis and that in our opinion it is fully adequate, in scope and quality, as a thesis for the degree of Master of Science.

_____

Assoc. Prof. Dr. Eray Uzgören
Supervisor

Examining Committee Members

Assoc. Prof. Dr. Eray Uzgoren	Mechanical Engineering Dept. METU NCC	_____
Asst. Prof. Dr. Murat Fahrioğlu	Electrical and Electronics Engineering Dept. METU NCC	_____
Assoc. Prof. Dr. Derek Keith Baker	Mechanical Engineering Dept. METU	_____

ETHICAL DECLARATION

I hereby declare that all information in this document has been obtained and presented in accordance with academic rules and ethical conduct. I also declare that, as required by these rules and conduct, I have fully cited and referenced all material and results that are not original to this work.

Name, Last name   :Kumudu Janani Gamage

Signature   :

ABSTRACT

NUMERICAL METHODOLOGY FOR FEASIBILITY ANALYSIS OF GROUND SOURCE HEAT PUMPS

Kumudu Janani Gamage

M.S., Sustainable Environment and Energy Systems Program

Supervisor: Assoc. Prof. Dr. Eray Uzgoren

Ground source heat pump (GSHP) systems provide an alternative energy source for residential and commercial space heating and cooling applications by utilizing the favorable temperature profile at a certain depth under the ground surface. GSHP's aftereffects on the ground temperature profile need to be considered for estimating the economical breakeven point. The present study develops a new semi-analytical model to analyze the short term response of the ground heat exchangers by accounting the depth dependencies in the heat transfer rates along the borehole. The model utilizes the solution of Kelvin's infinite-length line source theory to predict the borehole wall temperature but incorporates working fluid's inlet temperature to modify the heat transfer rate with time and depth to capture the borehole wall temperature variations in short time periods. The developed model is validated against other widely used short-term response models based on g-functions as well as three dimensional finite volume (FV) simulations, which can address the short-term transient behavior of the ground temperature response accurately but at high computational costs. The novelty of the model is that it is able to predict fluid's exit temperature for both short- and long-term periods without a need to explicitly consider load aggregation at a modest computational cost. The developed model is implemented on a case study for a dormitory building at METU NCC campus to investigate the economic feasibility of the proposed GSHP system by carrying out the breakeven point calculations against a conventional boiler for space heating applications. The study reveals that full sized GSHP system with a supplementary backup unit can economically break-even the GSHP installation cost after 4 years of GSHP installation with 470 ton CO_2 emission reduction.

Keywords: Ground Source Heat Pump, Ground Heat Exchangers, Line Source Theory, short-term thermal responses, OpenFOAM, break-even point

ÖZ

TOPRAK KAYNAKLI ISI POMPALARI FİZİBİLİTE ANALİZİ İÇİN SAYISAL YÖNTEM

Kumudu Janani Gamage

M.S., Sürdürülebilir Çevre ve Enerji Sistemleri Programı
Supervisor: Assoc. Prof. Dr. Eray Uzgoren

Toprak kaynaklı ısı pompası (ground source heat pump - GSHP) sistemleri, toprak yüzeyinin altındaki bulunan olumlu sıcaklık dağılımını kullanarak, konut ve ticari alanlarının ısıtma ve soğutma ihtiyaçlarını karşılamak için alternatif bir enerji kaynağı sağlamaktadır. Yeraltı sıcaklık dağılımı, GSHP'nin kullanımı ile değişmesi söz konusu olduğundan ekonomik başabaş noktasının tahmin edilmesi için kullanılacak yöntem büyük önem taşımaktadır. Bu tez, sondaj kuyusu boyunca derinliğe bağlı değişen ısı transfer oranlarını göz önüne alarak eşanjörlerin kısa süreli etkilerinin analizi için yeni bir yarı-analitik yöntem geliştirmektedir. Geliştirilen yöntem; sondaj duvar sıcaklığını, Kelvin'in sonsuz boyuta uzanan ısı kaynağı teorisinin çözümüne dayanmaktadır. Bu teoriden farklı olarak, kısa süreler içerisinde oluşacak sondaj duvar sıcaklığı değişimlerini yakalamak için zaman ve derinlik ile değişen ısı aktarım yoğunluğunu akışkanın giriş sıcaklığını kullanarak formüle etmiştir. Geliştirilen yöntem, yaygın olarak kullanılan g-fonksiyonlarına bağlı kısa dönem tepki yöntemleri ve detaylandırılmış üç boyutlu sonlu hacim (FV) simülasyonları ile karşılaştırılarak güvenirliği onaylanmıştır. Ayrıca, yöntem kısa ve uzun dönem hesaplarını, Kelvin'in sonsuz boyuta uzanan ısı kaynağı teorisini kullanan diğer yöntemlerin uygulamak zorunda olduğu yük toplama koşullarını dikkate almadan uygun bir süre içerisinde akışın çıkış sıcaklığı tahmin edebilmektedir. Geliştirilen model, GSHP sistemin ekonomik fizibilitesini araştırmak için ODTÜ KKK kampüsünde bir yurt binasının ısıtılması için kazan kullanımı düşünülerek karşılaştırılmıştır. Sonuç olarak, ek destek ünitesi ile birlikte tam boyutlu GSHP sistemi kullanıldığında, sistemin kurulum maliyetini 4 yıl içerisinde karşılayabildiğini ve bu süre içerisinde CO_2 yayılımını 470 ton kadar azaltılabileceği bulunmuştur.

Anahtar Kelimeler: Toprak Kaynaklı Isı Pompası, Toprak Eşanjörler, Çizgi Kaynak Teorisi, kısa süreli ısıl tepkiler, OpenFOAM, başabaş noktası

DEDICATION

To my Husband, Parents and Brother

For their unconditional support, trust and encouragement.

ACKNOWLEDGEMENTS

TABLE OF CONTENTS

LIST OF TABLES

LIST OF FIGURES

NOMENCLATURE

A	Aspect ratio
B	Borehole spacing (m)
COP	Coefficient of performance
C_{pf}	Heat capacity of the fluid (Jkg^{-1}K^{-1})
d_b	Borehole diameter (m)
d_e	Equivalent diameter for U-leg pipe (m)
d_{pi}	Inner pipe diameter (m)
d_{po}	Outer pipe diameter (m)
GHX	Ground heat exchanger
$GSHP$	Ground source heat pump
H	Borehole depth (m)
k_s	Thermal conductivity of soil (W/mK)
$\dot{m}$	Mass flow rate (kgs^{-1})
NB	Number of boreholes
Q	Heat transferred to fluid (W)
Q_C	Heat absorbed from the ground (W)
Q_H	Heat supplied by GSHP system (W)
q'	Heat flux at borehole wall (W/m)
r_b	Borehole radius (m)
R_b	Borehole thermal resistance (mK/W)
t	Time (hours)
t_s	Characteristic time (hours)
T_{amp}	Amplitude of the surface temperature (K)
T_b	Borehole wall temperature (K)
T_f	Fluid temperature (K)
T_∞	Undisturbed ground temperature (K)
$\bar{T}_s$	Mean ground surface temperature (K)
T_p	Penalty temperature (K)
z	Depth below the ground surface (m)

CHAPTER 1

INTRODUCTION

Ground source heat pumps (GSHP) provide significant benefits for space heating and cooling in buildings due to its capability of reducing energy consumption and CO_2 emissions by utilizing relatively stable ground temperature which remains constant at a certain depth below the ground surface and is always higher than that of the ambient air in the winter and lower than the summer [1] (Figure 1-1).
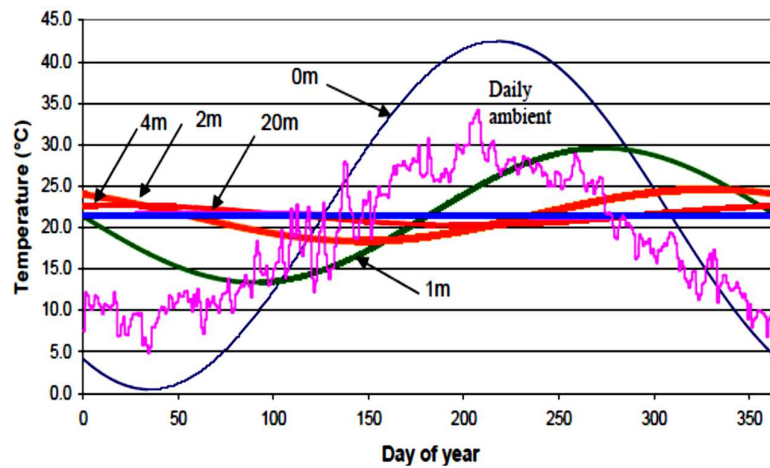
Figure 1-1 Temperature distribution of the ground [2]

Despite GSHPs aid in supplying heating and cooling needs of buildings, their use is still limited due to their high installation costs. GSHP system installation cost includes ground loop heat exchanger (GHX) installation cost and heat pump installation cost. To reduce the cost owing to installation of GSHP and enhance the savings from operational cost of GSHP system compared to conventional heating/cooling systems, proper sizing of GHX is important. Besides, designing a GSHP system is intricate by various case specific parameters, such as ground temperature profile, soil thermal properties, and buildings' cooling/heating loads.

Designing a reliable and an effective GSHP system requires the knowledge of GSHP's aftereffects on the ground temperature profile with cumulative effects of short-term responses. Owing to computational costs, many long-term simulation models neglect GSHP's hourly

transient behavior and assumed single fixed ground load within a user specified duration (days/months/years) causing over or under estimation of required size of the GHX system (length and number of boreholes) [3]. Actual heat transfer rates of GHXs show rapid oscillations due to changes in the hourly heating/cooling load requirements. These fluctuations, typically neglected by long-term models, are reflected in fluid temperatures going in and exiting the heat pump, which affects the energy consumption rate and system efficiencies [3]. Shot time step simulation models were introduced to eliminate these limitations in the long term simulation models.

Sophisticated 3-D numerical models that represent the exact nature of GHX were introduced for short time step simulations ([4] and [5]). These models can capture the actual heat transfer rates at the borehole wall as they can impose the non-uniform distribution in the undisturbed ground temperature and transient behavior of the ground surface temperature as boundary conditions which are assumed to be uniform or constant by the existing analytical models. However, they are only suitable for simulating the GHX for very short periods and not suitable for long term simulations as they are computationally very expensive.

Few analytical models can be found in the literature for evaluating the short term transient response of the GHX ([6], [7] and [8]) having capabilities for long term simulations. However, all of them assume a constant borehole wall temperature and constant uniform heat transfer rates along the borehole wall leading to large transient spikes in the exiting temperature of GHX in the case of sudden fluctuation in the building loads thereby causing errors in GSHP performance estimations [9].

The present study develops a GHX model capable of addressing short-term transient responses of GHXs at modest computational costs with intrinsic capabilities of accounting cumulative effects of short-term behavior for long-term analyses. The model predicts the transient variations in heat transfer rates at the borehole wall by utilizing the temperature difference between the non-uniform distribution of undisturbed ground temperature and fluid without a need to explicitly consider load aggregation at a modest computational cost.

A feasibility analysis of GSHP is also carried out on a case study develops at a dormitory building at Middle East technical university, Northern Cyprus campus to understand the economic and environmental benefits of GSHP over an existing conventional boiler for

heating purposes. The economic feasibility analysis considers the variation in the operational cost of the GSHP system due to sub hourly fluctuations in the heating loads, adaptation of fluids' exit and inlet temperatures to GHX in accordance with the hourly demand, uncertainty in the electricity and diesel prices and fuel and electricity price escalations. The effect of thermal degradation of GSHP system is discussed in terms of electricity consumption and the CO_2 emissions over the economic life time.

1.1 Thesis outline

The remaining part of the thesis consists of 5 chapters. Chapter 2 describes the basic principle of the GSHP system, its main components, existing GHX models, heating/cooling load estimation methods and GSHP system economics. Chapter 3 gives a detailed description about the scope and the objectives of the thesis. Chapter 4 discusses the development of new short time scale model for GHX, validation of the model against the literature and a fully developed three dimensional finite volume model. Chapter 5 conducts a feasibility analysis of GSHP on a case study develops at a dormitory building at Middle East technical university, Northern Cyprus campus against an existing conventional boiler for heating purposes. Chapter 6 finalizes the thesis by summarizing the achievements obtained from new semi analytical mode and feasibility analysis, and outlines the further study areas.

CHAPTER 2

BACKGROUND AND PREVIOUS WORK

GSHP system considered in this thesis consists of three main components, an earth connection subsystem, a heat pump subsystem and heat distribution subsystem. Figure 2-1 illustrates the main components of GSHP system. The earth connection subsystem is contained with a ground heat exchanger (GHX) which is used to exploit ground capacity for heating and cooling. Heat pump utilizes heat transfer between earth connection and heating/cooling distribution system [10]. This chapter gives a background information about GSHP subsystems and discusses about the previous research work on GSHP system and their limitations.
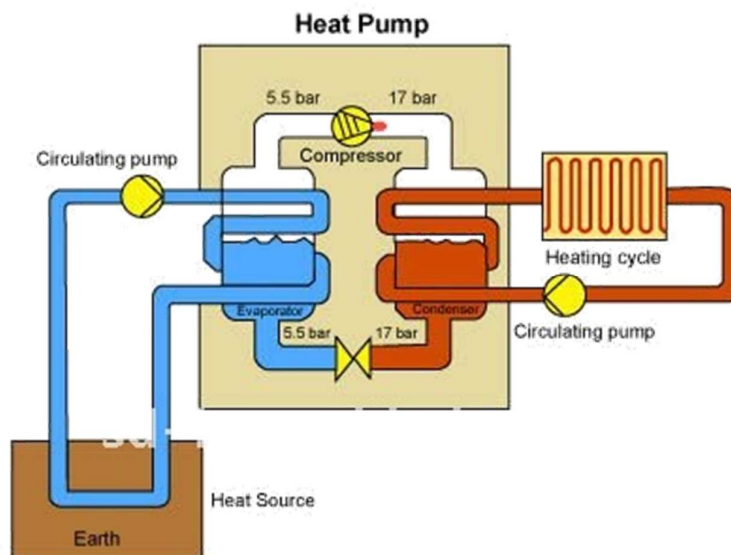
Figure 2-1 GSHP system components [11]

Section 2.1 describes the types of GHXs. Specifically, it focuses on the effect of various parameters on the GHX performance, existing long term and short term models for GHX modelling and their limitations. Section 2.2 describes about the heat pump sub-system and Section 2.3 discusses the novel GSHP technologies. Section 2.4 explains the calculation methods and existing software for heating/cooling loads of the building. Section 2.5 discusses about the existing feasibility analysis studies for GSHP systems.

2.1 Ground Heat exchanger

Earth connection subsystem consists of ground heat exchanger (GHX), which is typically formed in series of horizontally or vertically buried pipes. Depending on the type of the loop in ground heat exchanger, GSHP can be categorized into two groups as open loop and closed loop ground source heat pump systems.

- **Open loop ground source heat pump**

Ground-Water Heat Pump (GWHP) is another name for open loop GSHP. A schematic of GWHP is depicted in Figure 2-2 . GWHP uses underground water as a heat source or heat sink and it is connected to the earth through water wells.
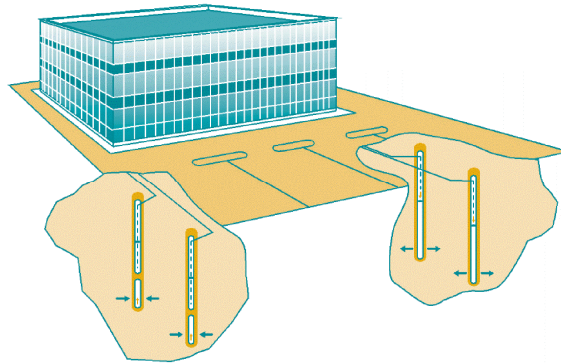
Figure 2-2. Open loop ground source heat pump [10]

These types of heat pumps are efficient and cost effective since there is no need for the deep excavation. GWHP needs significant amount of water with a reasonable quality. However, their main disadvantage is that it requires frequent cleaning to remove chemical precipitates or natural fouling which can damage heat exchanger [10].

- **Closed loop Ground source heat pump**

Ground coupled heat pump (GCHP) is also referred to closed loop ground source systems. Water or water/antifreeze solution is circulated through high density polyethylene pipe in vertical boreholes or horizontal trenches [12] as illustrated in Figure 2-3. These systems can be categorized into two groups as vertical and horizontal ground coupled systems.

(a)   (b)
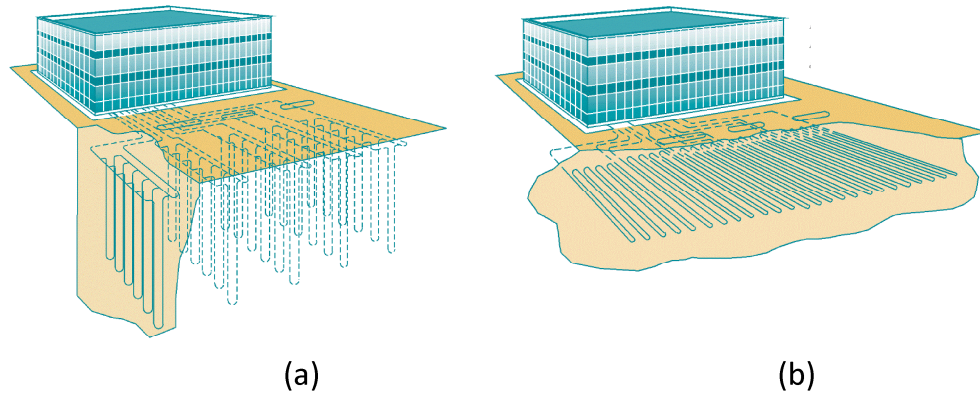
Figure 2-3. Closed loop Ground source heat pump (a) vertical loop (b) horizontal loop [10]

2.1.1 Types of ground heat exchangers

In horizontal GCHP systems, ground heat exchanger configuration consists of series of parallel pipes laid out in trenches dug about 1 m-1.8 m deep [12]. The main thermal energy source of the horizontal GCHP is the stored energy in earth due to absorbed solar radiation [13]. Therefore, it is important not to cover the surface above the ground loops where they are buried. Advantage of horizontal loop GCHP over the vertical loop GCHP is the lower drilling cost and flexible installation options [13]. Their disadvantages include large land requirement and low heat pump efficiencies due to temperature fluctuations of the ground which is sensitive to the daytime cycle of air temperature.

In vertical GCHP systems, ground heat exchanger consists of vertical boreholes in series [12]. Vertical loop GCHPs are used more for commercial installation where the bedrock is close to the surface and the space is limited. The depth of the boreholes, typically two pipes connected with a U-bend at the bottom, varies between 40 m and 150 m [10].Boreholes are filled with grout to prevent both draining of surface water into boreholes and leaking from one borehole to the adjacent borehole. This type of heat exchangers is very expensive compared to that of the horizontal type heat exchangers, but they are more efficient due to the fact that the pipes are buried deeper than the horizontal type GHXs and they can produce more stable exit temperatures. Design of vertical loop ground heat exchangers is complex due to the diversity of geological conditions. Proper sizing of the vertical loop GCHP system is crucial, specifically the depth of the borehole. Ground heat exchanger should not be too long which

can significantly increase the initial investment cost or it should not be too small which results in a deficit of energy demand. It is suggested that the piping requirement will be 60 m -185 m per ton of cooling capacity of a building [13].

GSHP can be further categorized into a third group as surface-water heat pump (SWHP). This type of GSHP can have either closed loop or open loop heat exchangers [12]. In the closed loop systems, heat is transferred by circulating a heat transfer fluid (HTF) through pipes located at a sufficient depth within a lake, reservoir or pond [4]. Since, the need for excavation in the installation of these systems is unnecessary, SWHP are inexpensive. Table 2-1 presents the summary of advantages and disadvantages of GSHP system technologies.

Table 2-1.Summary of the advantages and disadvantages of GSHP system technologies

Type	Advantages	Disadvantages
Ground-Water Heat Pump (GWHP)	• Efficient and cost effective since no need for the deep excavation	• Needs significant amount of water with a reasonable quality, • Frequent cleaning is required
Vertical closed loop (GCHP)	• More efficient than the horizontal heat exchangers	• High installation cost
Horizontal closed loop (GCHP)	• Lower drilling cost, • Flexible installation options	• Large land requirement, • Lower heat pump efficiencies
Surface-water heat pump (SWHP)	• No need for the excavation therefore, it is more inexpensive.	• Required significantly large water bodies

2.1.2 Thermal performance of ground heat exchangers

GCHP (vertical loop/horizontal loop) utilize the ground as a heat sink or a heat source. Thermal performance of GHX primarily depends on GHX ability to exchange the heat with surrounding soil. Heat transfer mechanism between the soil and the GHX depends on the local conditions, GHX design parameters and operation conditions [14], which impact their feasibility and economics of these systems. Local conditions include climatic conditions, hydrological conditions, thermal properties of the soil and ground temperature distribution [14]. GHX design parameters includes depth, U-tube shank spacing, pipe and borehole

thermal conductivities and diameters, velocity inside the pipes, fluid inlet-outlet temperature from the GHX, and bore-field configurations [14].

Ground temperature distribution directly affect the heat extraction and injection rates of the borehole as the difference between the ground loop and the soil temperature drives the heat transfer from ground to the GHX loop. Soil thermal properties also have a profound effect on the thermal performance of the GHX system [15]. Thermal response tests have been used as the primary methodology to determine the thermal properties of ground [16]. This is an in-situ test method which measures the temperature response of a fluid flowing through the GHX in a single borehole [12].

Thermal conductivity determines the rate at which the heat is transferred to loop from ground [17] making it a one of the key parameter to determine the length of the pipe and hence the installation cost of the GSHP system. Thermal conductivity of soil and rocks depends on lithology, porosity and the extent of saturation of soil [17]. Rocks rich in clay material have less thermal conductivity than rocks rich in quartz (like sandstone) [18].

Heat capacity of the soil determines the fluctuations in the ground temperature profile since it reflects the heat gain or loss per unit rise in the temperature. Both conductivity and heat capacity of the soil increases with saturation levels. Dry soil heat capacity is around one fifth of the wet soil. Therefore, light dry soil experiences high seasonal temperature variations at a given depth than wet soils [20] and hence, they are less reliable. Figure 2-4 depicts the temperature variation in the different type of soil as a function of depth below the ground surface.

Imbalances in annual heating/cooling loads cause thermal build up or depletion in ground heating/cooling capacity. Coefficient of performance of the GSHP system is reduced over the time of operation leading to greater length for ground loops. Due to a considerable groundwater flow, heat buildup at the borehole area can be minimized and can avoid the over-sizing of the ground heat exchanger [19].

When looking at the effect of GHX parameters into the thermal performance of GHX system, length of the borehole system plays an important role. Deeper the loop installed, higher the coefficient of performance of the heat pump is. This is due to the ground temperature at the

deeper layers is approximately equal to the annual mean air temperature [17] and makes the temperature difference between the heat source and heat sink smaller. As a result, annual operating cost decreases while the depth of the ground loop increases, so does the capital cost of the GSHP system.
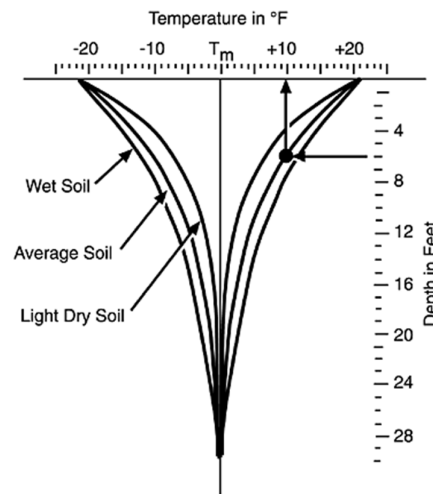
Figure 2-4 Temperature variations in the different type of soil as a function of depth below the ground surface [20]

Effect of geometrical parameters on the thermal performance of the GHX is a measure of borehole thermal resistance [21] which can be determined by the thermal response test data. Borehole thermal resistance indicates the temperature drop between the undisturbed ground and fluid in the pipes [1]. Higher borehole thermal resistances leads to decreased thermal performances of GHX. Velocity in pipes, U-tube shank spacing, grout thermal conductivity, and fluid inlet temperature to GHX are the principal factors which determine the borehole thermal resistance. Rise in the velocity in pipes reduces the convective thermal resistance of borehole. Even though its contribution into the total borehole resistance is less than 1%, smaller changes in velocity effect the heat exchange rates at the borehole significantly [14]. Decrease in the U-tube shank spacing enhances the thermal interference among U-loop, thereby reduces the heat transfer rates. When thermal conductivity of the grout is increased, total borehole resistance is also decreased and hence, heat transfer rates considerably increased [14]. It has also been found that, higher inlet temperatures in summer leads to

9

greater heat transfer rates as the difference between the soil and fluid temperature is increased. However, it is the opposite in winter [14].

Another factor that causes the thermal performance of GHX is the thermal interaction among the boreholes. In case either heating load or cooling load dominates each other over the years of operation of GHX, so called thermal inference among the boreholes needs to be accounted as this causes significant changes (increase or decrease) in the ground temperature. Thermal inference can reduce the thermal performance in the GHX system [22]. For example, consider a 3×3 configuration of bore-field as illustrated in Figure 2-5. For space cooling applications in summer, heat diffused from 8 neighboring boreholes interact with the heat diffused from the borehole at the center of the bore-field and thereby trap the heat at the bore-field center. Similar condition occurs for the remaining boreholes causing significant increase in the ground temperature over the time [22]. Long term temperature changes in the ground due to this thermal interaction among the boreholes is a three dimensional concept and it is computed by evaluating the effective increase (or decrease) in the undisturbed ground temperature over the time. The effective temperature changes in the ground is called as the penalty temperature (T_p) and it depends on the borehole spacing (B), number of boreholes in the bore-field (NB), depth of each borehole (H), aspect ratio (A) which is the ratio of number of boreholes in the longest direction of the bore-field over number of boreholes in the shortest direction. A detail description of GHX thermal performance on bore-field configurations can be found in Bernier et al. [22].
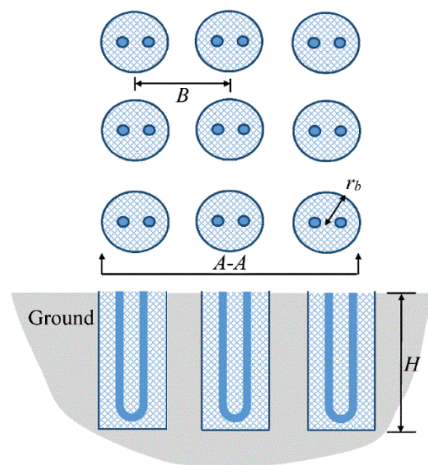
Figure 2-5 Schematic representation of a bore-field with 3×3 configuration

2.1.3 Ground heat exchanger models

Vertical loop ground heat exchangers are more efficient than the horizontal loop ground heat exchangers in terms of thermal performance and they are suitable for any kind of building's (commercial and residential) heating/cooling applications as they require smaller land area. However, as discussed in the previous section, the design of vertical loop ground heat exchangers are intricate by diversity of geological, hydrological and operational conditions. Therefore, for proper sizing and energy analysis of vertical loop GHX system, study of long term and short term behavior of ground heat exchangers are important [23].

The existing models for GHX simulations can be categorized mainly as long time scale GHX simulation models and short time scale simulation models. Depending on the methodology they used for the simulations, they are sub categorized as analytical, numerical and response factor models [24].

- **Long time scale GHX simulation models**

Sustainability of ground heat exchangers are mainly depended on its capability to reject or extract the heat from the ground over the years of operation and the prevention of the thermal build up or depletion of the bore-field [23]. Therefore, long time scale GHX models are usually used for designing purposes. Specifically, they are used for sizing the length, number of borehole and spacing between the boreholes in the GHX system as they require less computational time and sometimes do not require any costly computations [25]. These long time scale GHX simulation models usually use monthly building loads for system design and offer monthly average water entering and existing temperatures to the heat pump. Some models even use peak load for this purpose [3]. However, long time scale GHX models are not suitable for detail energy analysis and or system controls applications [3].

Long term time scale models usually ignore the thermal resistances inside the boreholes. However, as thermal buildup in the far-field is significant compared to the local borehole thermal distribution, effect of these simplifications into the analysis of changes in the ground performance are insignificant [23].

Analytical models are much more efficient in terms of computational cost than the numerical models for long term ground heat exchanger simulations. Among the existing analytical

models, Kelvin's infinite-length line source theory [26] and infinite-length cylindrical source theory, developed by Carslaw and Jaeger [27] are very popular in the literature for long time scale GHX modeling. The line source theory assumes that vertical loop GHX as an infinitely long line source with radial heat flow whereas infinite cylindrical source theory assumes it as a hollows cylinder. Both predict the radial and temporal distribution of ground temperature assuming constant thermal properties and constant step heat pulse along the borehole wall. They neglect the variations in the undisturbed ground temperature profile along the depth and thermal capacitance of the borehole elements. The changes in the ground loads over the time is accounted by temporal superposition techniques.

Eskilson et al. [28] developed a long time step response factor (g-function) model to simulate borehole fields with defined configurations over long timescales, ranging from one month to several years. These response factor models use hybrid approach which combines both analytical and numerical methods. The methodology of developing response factors for multiple borehole system includes two steps. First, 2-D finite difference simulations are carried out for a single borehole to determine the temperature response of the borehole wall due to unit step heat pulse. This step heat pulse is assumed to be constant along the borehole. The spatial superposition method is then used to find the thermal response of a defined bore-field due to multiple boreholes. For a constant unit heat transfer rate q' (W/m) per unit length, g-function for entire bore-field with n number of boreholes can be written as follows [22],

$$g_n(t/t_s, r_b/H, B/H, \text{borefield geometry}) = \frac{2\pi k_s(\overline{T}_{b,n} - \overline{T}_s)}{q'} \qquad (1)$$

Where, g_n represents the g-function (non-dimensional response factor) for n boreholes, r_b is the borehole radius (m), H is the depth of a single borehole (m), t is the time (days), t_s ($=H^2/9\alpha_d$) is the characteristic time (days). α_d represents the thermal diffusivity of soil (m^2/day), B is the borehole spacing (m), k_s is the thermal conductivity of soil (W/mK), $\overline{T}_{b,n}$ is the average borehole wall temperature for n boreholes (K), $\overline{T}_s$ is the undisturbed mean ground temperature (or mean surface temperature).

As the line source theory and the cylindrical source theory, Eskilson's g-function model also neglects the thermal resistances owing to borehole elements and calculates only an average

output for borehole wall temperature and variations in the ground load over the time is accounted using the temporal superposition techniques.

Eskilson has estimated more than 200 g-functions for multiple borehole system with different configurations. These g-functions have been implemented in commercial software called "GLHEPRO"[29]. Later, Bernier et al. [22] has introduced a correlation function for Eskilson's g-function performing a linear regression analysis for large number of g-function curves corresponding to different set of bore-field configurations. In his model, concept of temperature penalty was introduced to account the real response of ground due to thermal interference among the boreholes. The borehole sizing equation that he developed, accounts the effect on ground response due to three successive thermal pulses (yearly, monthly and annually) on ground and uses cylindrical source theory to calculate the transient ground resistance due to these three thermal step pulses.

As described above, all these analytical and hybrid models calculate the ground temperature response for constant step heat pulse (load) along the borehole wall and account the varying ground load over the time by temporal superposition techniques [30]. Several temporal superposition techniques can be found in the literature for both short time scale and long time scale GHX models [31], [32] .

Simple temporal superposition techniques include non-aggregated superposition techniques. In these methods, time varying ground load $Q(t)$ (W) is discretized into several constant load steps over the time as Figure 2-6. Then, total changes in the borehole wall temperature over the time is calculated by taking the summation of outcome of each single step load [30]. Mathematically, this can be illustrated as follows,

$$\overline{T}_b = \overline{T}_s + \frac{1}{LCk_s}\sum_{i=1}^{N}Q'_i(G(F_0(t_N - t_i)) \tag{2}$$

where, $\overline{T}_b$ is the average borehole wall temperature, $\overline{T}_s$ is mean ground temperature (or mean surface temperature), C is a generic constant which is selected based on the analytical model selected (either line source theory or cylindrical source theory). L is the length of the borehole. k_s is the ground thermal conductivity, G is the generic thermal heat transfer function which

depends on dimensional time F_0, Q' is the corresponding superimposed load for step ground load (W). t is the time and N is the number of different step heat pulses.
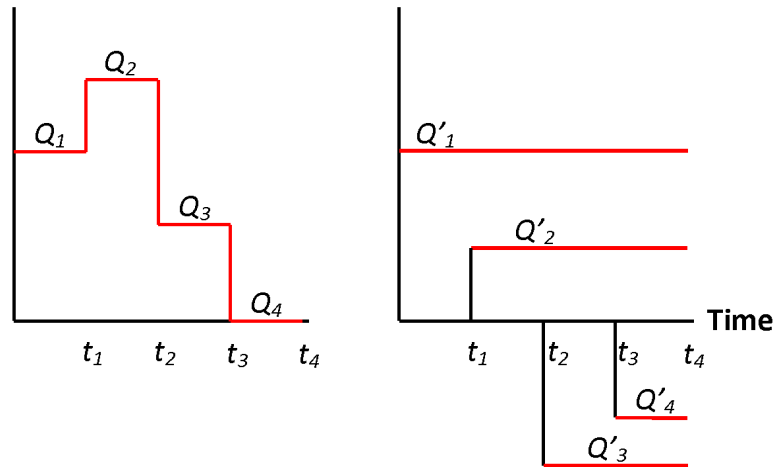
Figure 2-6. Temporal superposition of ground heat step pulses (a) Discrete ground heat pulses (b) Temporally superimposed ground step pulse on time

- **Short time scale GHX simulation models**

Vertical loop GHX models for short time scale (hourly or less) play an important role in direct assessment of the energy consumption of the ground source heat pump (GSHP) system. Actual heat transfer rates from (to) ground heat exchangers (GHX) oscillates rapidly due to changes in the hourly heating/cooling load requirements. Therefore, results in fluctuations in the inlet fluid temperature into the heat pump [3]. These fluid temperature variations have a direct impact on the coefficient of performance of the heat pump (COP), and hence effect the energy consumption and the system efficiencies, which makes the short term behavior of the GHX with hourly or sub hourly intervals very important.

Several analytical and numerical models for modeling the short term behavior of GHX can be found in literature [33], [34] and [35]. Among these models, detailed numerical models using either finite volume (FV) or finite element (FE) can predict short term fluctuations in the fluid temperature and capture heat transfer rates accurately at a high computational cost. This is primarily due to the fact that they can handle the geometry related complexities and

temporal-spatial variations in the boundary conditions precisely compared to the analytical models.

Li and Zheng [4] developed a three dimensional finite volume model to predict hourly existing fluid temperature of the ground heat exchangers. Transient heat conduction through the soil, pipe and grout, convection heat transfer in the pipe inner surface and fluid is modeled. Their model uses Delaunay triangulation method to mesh the borehole in order to model the geometry accurately and considers a uniform undisturbed ground temperature distribution. Khalajzadehet et al. [5] proposed a methodology to optimize the design parameters of vertical loop GHEs using a three dimensional computational fluid dynamic model developed using FLUENT software. They have optimized the parameters of the GHX based on the heat exchanger efficiency and the total heat transfer efficiency. Unlike the other numerical models, they have taken into account the actual variations in the undisturbed ground temperature profile along the depth.

Yavuzturk and Spitler [3] developed a two dimensional finite volume (FV) model to compute non dimensional ground temperature response in short time scale (short time step g-functions). In his model, shape of the U-tubes was approximated by pie sectors and assumed constant heat flux along the borehole wall. Variations in the undisturbed ground temperature profile and non-uniform heat transfer rates along the borehole were neglected. Therefore, average borehole wall temperature is used to calculate the inlet and outlet temperature for heat pump. Thermal properties of the materials inside the borehole were modeled since, borehole local effect are important in short time scale simulations. Their method of developing short time step response factor is an extension of the previous work of Eskilson's long term g-functions. First as the Eskilson's long term g-function calculation method, FV model calculates the changes in average borehole wall temperature compared to undisturbed ground temperature due to a single step heat pulse and non-dimensionalized it to form the short time step g-functions. Unlikely long time scale simulations, number of time steps that need to account for the temporal superposition of ground loads are huge. Consequently, usual temporal superposition techniques use in the long time scale are computationally expensive. Therefore, Yavuzturk and Spitler [3] suggested that load happening after a certain time ago can be lumped together into larger blocks. Then, average ground load over the time and depth is calculated for user definable loads subjected to the significance of the load at a given time, thereby reduce the computational time need for simulations [3].

15

Even though, numerical models in [4] and [5] can accurately predict the transient behavior of outlet temperatures of GHX, analytical models are always superior to the numerical models in terms of computational cost and flexibility. Nevertheless, line source theory and cylindrical source theory were used originally for long time scale of GHX medelling, they were later used for short time scale modeling as well by introducing the thermal resistances concept inside the borehole to account the heat transfer between fluid and the borehole wall which are important in short time scale GHX modelling. Nagano et al. [6] ,Yang et al. [7] and Wang and Qi [8], have simulated the short term performance of the GHX at hourly basis with integrating the borehole thermal resistances into line source and cylindrical source theory. All of those analysis, assumed that undisturbed ground temperature is uniform along the depth and heat flux along the borehole wall is constant which leads to constant borehole wall temperature along the depth. The time varying heat flux along the borehole in their models were accounted using temporal superposition techniques.

Assumption of average borehole wall temperature and constant heat flux along the borehole wall that use in the existing analytical models can cause errors in the calculation of fluid's outlet temperature of GHX in case of sudden changes of inlet temperature [9] . Therefore, Olfman et al.[36] has recently evaluated the validity of these assumptions for modeling the GHX by conducting an experiment on a site at University of Manitoba's Fort Garry campus, Canada. Temperature measurements at several depths along the observation wells near the borehole showed that temperature response of the GHX changes with the depth significantly. Furthermore, parametric study followed by his experiment illustrated that some regions of the boreholes are ineffective and therefore it is necessary to take into account the variations in the ground temperature distribution and thereby incorporates the actual heat transfer rates along the depth for designing and simulating the GHX responses for short time. Therefore, this thesis will address these limitation in the existing analytical models which assume uniform ground temperature distribution and constant heat flux along the borehole wall by utilizing the temperature difference between fluid and the non-uniform undisturbed ground temperature distribution.

2.2 Heat pump

The second main component of the GSHP system is the heat pump. Air conditioners and heat pump has the same characteristic of ability to transfer the heat from low temperature medium

to high temperature medium. But, their objectives are different. An air-conditioner extracts the heat from inside the building and dumps it outside of the building while a heat pump takes heat from outside of the building and releases it to the inside of the building to provide heating [37]. Examples of common heat pumps are gas compression heat pumps, phase change heat pumps, thermoelectric heat pumps and geothermal exchange heat pumps [13]. Current heat pumps are built combining both cooling and heating capabilities to serve as air-conditioner and heat pump. This dual mode of the heat pump system is controlled by switching the flow direction of the refrigerant [38]. Heat pumps can be categorized into three main groups depending on their heat source or sink and their distribution fluid such as air-air, water-air and water-water [37]. Heat pump collects heat from air, water, or ground outside the conditioned space and transfers it to inside of the buildings. Air-source heat pump uses air as the heat source or sinks whereas GSHP system uses water as their heat source or sinks which exchange the heat with earth or water bodies such as lakes, ponds and ground wells. This source water is generally combined with some anti-freeze solution such as ethanol, methanol and glycol [39]. Inside the conditioned space, heat can be transferred through water or air depending on the distribution system [37]. The ideal vapor-compression refrigeration cycle is used to describe the heat transfer process of air-conditioners as well as heat pumps. The cycle is consisted of circulating refrigerant and four major components including evaporator, compressor, condenser and expansion valve. The schematic of refrigeration cycle of a typical heat pump is shown in the Figure 2-7.
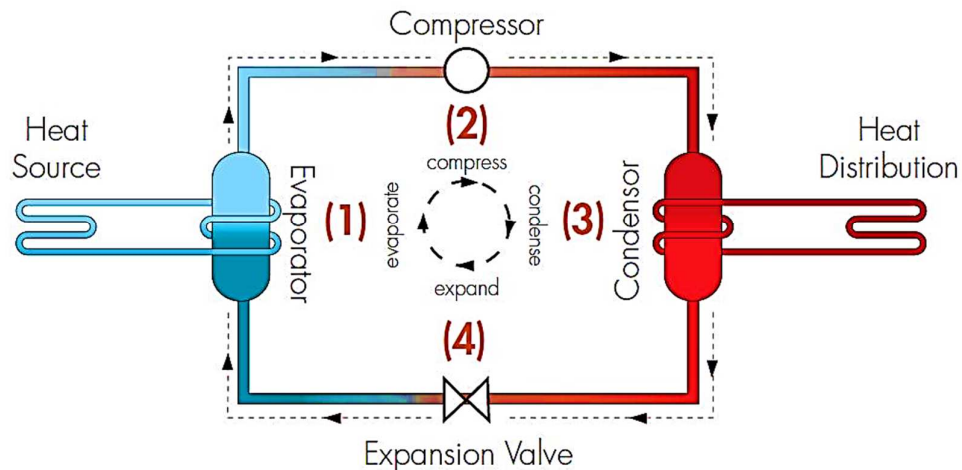
Figure 2-7 Schematic of refrigeration cycle of a typical heat pump [40]

Every ideal vapor compression cycle has four processes: isentropic compression in the compressor (1-2), constant-pressure heat rejection in the condenser (2-3), throttling in the expansion device (3-4), and constant-pressure heat absorption in the evaporator (4-1). The changes in thermodynamic properties of each process of cycle are depicted in the temperature to entropy (*T-S*) diagram (Figure 2-8).
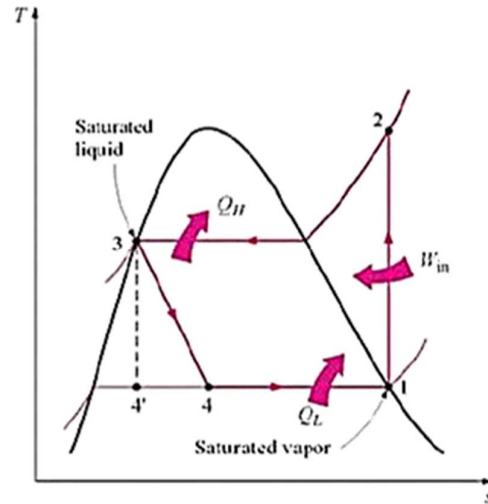
Figure 2-8 Absolute temperature to entropy (*T-S*) diagram [41]

In the heating mode of the GSHP, cold refrigerant absorbs the heat at the evaporator and leaves it as a low pressure low temperature saturated vapor. This gaseous, low pressure and low temperature refrigerant then passes into an electrically-driven compressor and then compressed into the compressor pressure (1-2). The refrigerant enters the condenser which is the coils in the conditioned space, as a superheated high pressurized vapor and cools down by rejecting heat to the conditioned space (2-3). Then, refrigerant leaves the condenser as a high pressure and medium temperature liquid. The pressure of the refrigerant is reduced when it passes through the expansion valve and leaves the same as low pressure low temperature liquid which is below the temperature of the conditioned space (3-4).The cooling option of the same cycle can be obtained by switching the indoor from heat sink to heat source [37].

The performance of a heat pump can be determined by the coefficient of performance (COP). COP is the ratio of the rate of removal or delivered heat to the conditioned space and the

energy input. COP_R is the COP of the refrigeration and COP_{HP} is the COP of heat pump. Derived equations for the COP_R and COP_{HP} are given in Equation (3) and (4) respectively.

$$COP_R = \dot{Q}_L / \dot{W}_{net,in} \qquad (3)$$

$$COP_{HP} = \dot{Q}_H / \dot{W}_{net,in} \qquad (4)$$

Where $\dot{Q}_L$ and $\dot{Q}_H$ is the rate of heat removal from the conditioned space and rate of heat delivered to the conditioned space respectively. $\dot{W}_{net,in}$ is the net rate of energy input.

Ground source heat pump has higher COP values than the conventional heating and air-conditioning systems. In the heating mode, GSHP can obtain COP in the range of 3-5 [13] depending on the ground temperature profile and the thermal conductivity of the soil, whereas conventional heating and air-conditioning systems have COP of less than 1 (Electrical resistance heating system has COP of 1, oil heating has 0.65-0.7 and high efficiency natural gas heating system has 0.8-0.9) [42]. Heat pump COP values vary with heat source or sink temperature. Air-source heat pumps are subjected to the higher temperature fluctuations due to the ambient air temperature variations. They become much less efficient at extreme ambient air temperatures. In addition, using air as the heat transfer medium is not effective as the water, due to low thermal capacity of air. GSHP uses water as its medium of heat transfer and ground as the heat source. Temperature below the ground surface does not fluctuate significantly through the day or in the year, as the air temperature. Ground below about 12m, the temperature is remained constant throughout the year [18]. GSHP remain extremely efficient throughout the year in any climate [13].

2.3 Novel technologies for GSHP

Due to the imbalances in heat extraction and rejection from/to ground, ground temperature near the borehole may change and result a less performance of the heat pump. For regions with dominating heating loads, without, extra heat injection in to the ground in the summer, ground temperature is decreased and may fail to supply the required heating load in the cold winter. Therefore, novel hybrid GSHP system technologies have introduced to overcome these problems. Wang et al [8] and Yang et al.[7] have proposed novel hybrid GSHP systems which use solar and earth as heat source for heating dominated regions. The proposed solar

assisted ground source heat pump in Yang et al. [7] is operated in two modes, alternate mode and combined mode. In the alternate mode, solar assisted heat pump works in the day and GSHP is operated in the evening or in the rainy days. In the combined mode, solar assisted heat pump and GSHP is worked simultaneously. Figure 2-9 illustrates the schematic of the solar assisted ground source heat pump proposed by Yang, et al. [7]. Gan et al. [43] has also proposed a novel GSHP system which uses rainwater and ground as heat source or heat sink. Rain water is used as a heat source for the GSHP by employing a heat exchanger into a water storage tank and the surrounding soil. This method, minimize the need for the drilling and so is the installation cost.
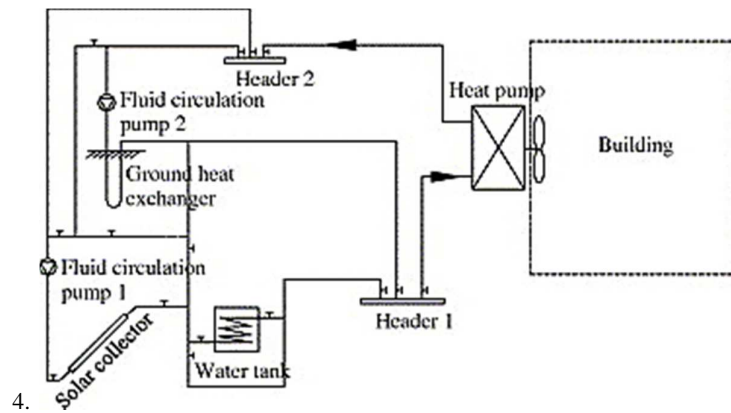
Figure 2-9. Schematic diagram for solar assisted ground source heat pump [7]

2.4 Heating/cooling load estimation methods

Heating and cooling load calculation is a very important step in determining the design parameters of the GSHP system. The amount of heat rejection/extraction to/from the ground are depended on the building loads. Heating load is determined by the heat loss of the building during the winter season and cooling load is the heat gain of the building during the summer. Heat gain of a building is resulted due to internal and external sources of the building. Internal sources of heat gain are lights, people, equipment, etc. External heat gain is resulted from heat gain from outside sources of the space. These include conduction heat gain through windows, walls, ceilings, and roof, sensible heat gain through windows and walls, infiltration heat gain through cracks in the building envelope. Figure 2-10 represents the sources of cooling and heating loads of a building.
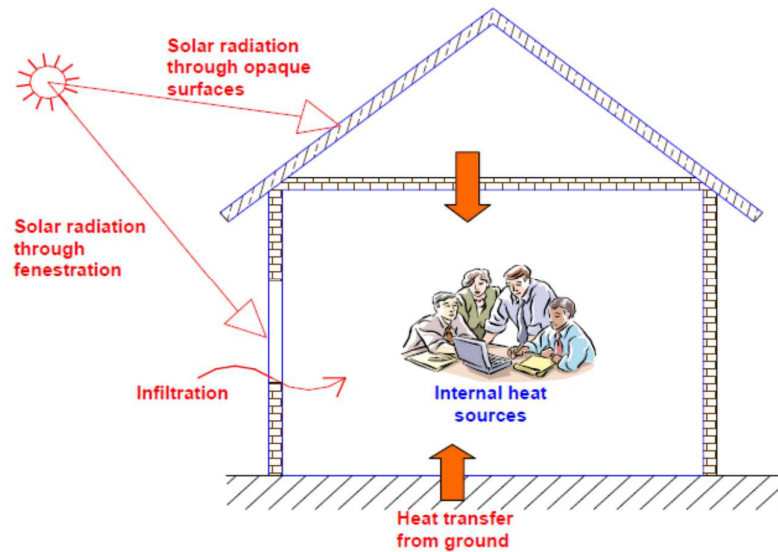
Figure 2-10 Sources of building heating/cooling loads [44]

Before computer aided building simulation software introduced, building service engineers and architects were mainly relied on the simple "hand" calculation methods such as degree-day method, equivalent cooling days and Bin methods [45]. However, theses simplified methods do not account the dynamic behavior of the building outdoor and indoor conditions such as variations in the occupant schedules and climatic conditions [45] and therefore not suitable for large or complex building load simulations.

Today, several computer aided building load simulation software can be found and their use is essential for energy-efficient design of HVAC systems for large complex buildings [46]. The available computer aided building load simulation software can be categorized as open source code and commercial programs [45]. Example of open source software are DOE-2, ESP, EnergyPlus, OpenStudio, and BLAST. TRNSYS is an example of commercial software package. These all software packages have the capability to simulate hourly building loads and takes the weather data, building location and building description, AC system data as the inputs [45]. These dynamic simulation models use different thermal modeling techniques such as energy balance method, transfer function method and finite difference method.

Commercial software packages are very expensive and they includes several cost components such as software cost, license fee, upgrading fee and training cost [46]. Therefore, when

selecting a building simulation model, the user should concern about the purpose, budget and available computer facilities [46].

2.5 GSHP economics

Ground source heat pumps provide significant benefits to the space heating and cooling applications due to its less energy consumption and the reduction in CO_2 emissions [14]. Ground source heat pump technology has been gaining attention in the renewable energy research field. Nevertheless, its usage is still limited as the installation cost is very high compared to the existing conventional space heating and cooling appliances [14]. In order to promote the GSHP system for residential and commercial building's cooling and heating applications, customers of GSHP need to understand the economic and environmental benefits of a GSHP system.

There are number of ways to analyze the economic feasibility of using GSHP system. Some of them are payback period calculation method, life-cycle cost analysis method, net benefit (present worth) method, savings-to-investment ratio method, internal rate of return method and analytical hierarchy process [47].

Several economic feasibility analysis on GSHP system can be found in the literature [30] ,[48], [6] , [49], [34], [7] and [50]. Doherty et al. [51] has investigated the economic feasibility of replacing the existing gas condensing boiler in an Eco-House at the University of Nottingham by a vertical loop GSHP system for purpose of space heating application. Heating load was calculated using both degree-day and Bin method. Vertical loop GHX was installed at the Eco-house based on the maximum heating requirement of the building (8 kW). Control systems were installed to monitor the ambient air temperature changes, ground temperature and inlet and outlet temperature of the GHX. Based on the experimentally collected outlet temperature data, average value for COP was calculated. Average annual heating energy consumption of the building was estimated assuming a constant 12 hour operation of GSHP system per each heating degree day over a year with the maximum peak load. Payback period of recovering the additional cost of installing the GSHP system over the gas fired boiler was 5.71 years. The reduction of CO_2 emission using GSHP over the gas fired boiler was 3.8 tons per year. Hourly changes in the ground temperature, heat extraction rates of GHX, fluid temperature and COP were not included into the operational cost calculations rather constant

values were assumed. Uncertainty and the cost escalations in the gas and electricity prices were not considered, but simple payback period calculation was used.

Petit and Meyer [52] has compared the economic benefits of installing horizontal loop GSHP system over air source heat pumps in South Africa. The analysis included the simple payback period, NPV and interest rate of return calculations for replacing an existing air-source heat pump system by horizontal loop GSHP system. In order to find the optimal depth for horizontal loop GHX installation, economics of installing GHX at different depth below the ground were studied. Capital cost is calculated based on the total length and volume of soil need to be excavated for GHX installation. Total length for GHX loop at various depths was estimated based on ground temperature distribution relationship to heat extraction capabilities of ground. The operational cost of Air-source heat pump and the ground source heat pump were calculated based on monthly average COP values for heat pumps and heating capacities of air and ground. NPV calculations were carried out with assuming constant annual savings over the life time. Electricity price escalations over the time period were ignored. The study concluded that GSHPs are more feasible than air source heat pump system for South Africa's climate.

Esen et al. [53] has studied the economic feasibility of installing a horizontal loop GSHP system in Turkey against five conventional heating method including electric resistance, fuel oil, petrol, natural gas, diesel and coal. Annualized levelized cost method was used to calculate the cost effectiveness of the GSHP system over the conventional heating methods. The operational cost of the heating system was accounted with the fuel escalation and inflation rates. The economic analyses is conducted assuming constant annual electricity consumption in GSHP system. Payback period of the GSHP against the electric resistance, diesel, petrol, coal, fuel oil and natural gas are 8.38, 10.31, 12.43, 20.75, 23.17 and 35.68 years respectively.

Blum et al. [54] has evaluated the technical and economic factors that affect the energy performance and design of vertical loop GSHP systems in Germany. The analysis was performed based on the real statistical data of 1100 GSHP systems installed throughout Germany. Based on the collected data, linear correlation was found for heating demand vs capital installation cost and exponential correlation was found for heating demand vs total borehole length. However, no correlation between the design of GSHP system and the ground characters in the Germany was found. Therefore, author suggested that ground thermal and

physical characteristic were not effectively utilized during the design and installation phase of GSHP systems which has led to under or oversized the system. Their study also revealed that distribution of cost parameters and heat exchange rates even within a single country can vary significantly and therefore, it is necessary to include the uncertainty when economic aspects of GSHP system are studied.

Garber et al. [47] has proposed a probability based approach to compare the cost effectiveness of the GSHP system as opposed to the conventional HVAC systems. The analysis showed that savings from GSHP system mainly depend on HVAC system efficiencies and gas and electricity prices. Transient system simulation program (TRNSYS) was applied to model the performance of GSHP system and calibrated the model with actual data from a hybrid GSHP system installed at the Department of Earth Science, University of Oxford, UK. Uncertainty in the lifetime operational cost of each HVAC system and installation cost were accounted using Monte Carlo simulations. The total lifetime of CO_2 emissions of conventional HVAC systems and the GSHP were calculated and shown that there is a potential of reducing the emissions when GSHP system is used. However, the analysis has not clearly discuss about the reduction of GSHP system performance over the years of operation and their effect into NPV calculations.

CHAPTER 3
SCOPE AND OBJECTIVE OF THE THESIS

It is observed from the literature review that a significant amount of research has been conducted on vertical loop ground heat exchanger modelling. Even though, sophisticated three dimensional numerical models can be found in literature for modelling the transient behavior of GHXs, they are computationally very expensive. Few studies can be found that use the analytical models for short time scale modelling of GHXs. However, none utilize the difference between fluid temperature in the pipes and non-uniform ground temperature distribution along the borehole to calculate the fluid's exit temperature, but rather they assume uniform ground temperature distribution along the borehole depth for the fluid temperature calculations which can lead to large transient spikes in the fluid's exit temperature in case of sudden fluctuations in the hourly heating and cooling requirements of the building. These assumptions can cause errors in the GSHP system performance calculations and energy consumption calculations. Therefore, it is necessary to develop a short time scale semi-analytical model that can simulate the GHX exist fluid temperature by accounting the non-uniform ground temperature distribution. Also, for the long term performance analysis of the GSHP system, the model should have the intrinsic capabilities of accounting the cumulative effects of short-term behavior of GHX for long-term analyses with less computational cost.

Further, in order to popular the GSHP technology among the people, performing a feasibility analysis against the conventional heating/cooling is important, as it is the only way to encourage the people to install GSHP technology by knowing their benefits in terms of reduced operational cost and environmental benefits. However, as seen in the literature, existing feasibly analysis methods do not address the real thermal behavior of GSHP along its long life operations, but rather assume constant performance or not properly describe their effect on break-even point calculations. To address this issue, a numerical methodology for feasibility analysis of GSHP system is introduced. The model will utilize the hourly or sub hourly thermal performance of GSHP system and their after effects on long term thermal behavior of GHSP for NPV an break-even point calculations.

The contribution of this study can be summarized as follows,

1. Develop a new semi-analytical model to analyze the short term response of GSHP system by utilizing the temperature difference between the fluid and non-uniform distribution of undisturbed ground temperature without a need to explicitly consider load aggregation.
2. Validate the semi-analytical model against the existing short term ground temperature response model in the literature and a three dimensional finite volume (FV) model.
3. Develop a numerical methodology to analyze the feasibility of GSHP system compared to conventional heating /cooling systems and implement it on a case study for dormitory building at METU, NCC.

CHAPTER 4

VERTICAL LOOP GROUND HEAT EXCHANGER MODEL

In this chapter, a new semi-analytical model is developed to evaluate the temperature response of a vertical loop ground heat exchangers (GHX) for short term periods, which play an important role in direct assessment of the energy consumption of the ground source heat pump (GSHP) system. The model considers the analytical solution of the line-source theory applied on a 1D depth-wise discretized space. Unlikely the existing analytical models for GHX, this model utilizes the difference between fluid temperature and non-uniform ground temperature distribution along the borehole to capture the actual direction and magnitude of heat transfer rates at the boreholes. The novelty of the model is that it is able to predict fluid's exit temperature for both short- and long-term periods without a need to explicitly consider load aggregation at a modest computational cost. The model is validated against the existing short term ground temperature response model in the literature and a three dimensional finite volume (FV) simulations, which also address the transient behavior of the ground temperature response in sub-hourly intervals at high computational costs.

Section 4.1 describes the development of a new semi-analytical model to evaluate the GHX responses for short term periods. Section 4.2 explains the development of a detailed 3D finite volume model for transient analysis of GHX's short term responses. Section 0 presents results and discussion of the developed model. Finally the chapter ends with a summary.

4.1 Semi-analytical model

For a constant heat flux at the borehole wall, borehole wall temperature can be calculated by applying line source theory or cylindrical source theory. As the pipes in the borehole system are usually very small and implementation of line source theory is easier than the implementation of the cylindrical source theory, this model uses line source theory as the basic theory for modeling GHX. Based on line source theory, Equation (5) can be used to calculate the borehole wall temperature for a constant heat flux at the borehole wall. As the far-field temperature of the ground (undisturbed ground temperature) is varied with depth, heat flux at the borehole is also varied with depth. Therefore, in order to use Equation (5) to

calculate the borehole wall temperature at a given depth, borehole is discretized into several layers as shown in Figure 4-1 and apply the line source theory at each layer separately.

$$T_b(t) = T_\infty(t) + \frac{q'}{4\pi k_s} \int_{r_b^2/4\alpha_s t}^{\infty} \frac{e^{-u}}{u} du \qquad (5)$$

where, T_b is the borehole wall temperature (K), T_∞ is the undisturbed ground temperature (K), q' is the heat exchange rate at the borehole wall (W/m), r_b is the radius of the borehole (m), k_s is the thermal conductivity of the soil (W/mK), α_s is the thermal diffusivity of the soil (m^2/hr), t is the operation time of GSHP (hr), u is the integral variable. In Equation (5), the heat exchange rate, q' has a negative value when the ground is cooled by the heat pump.
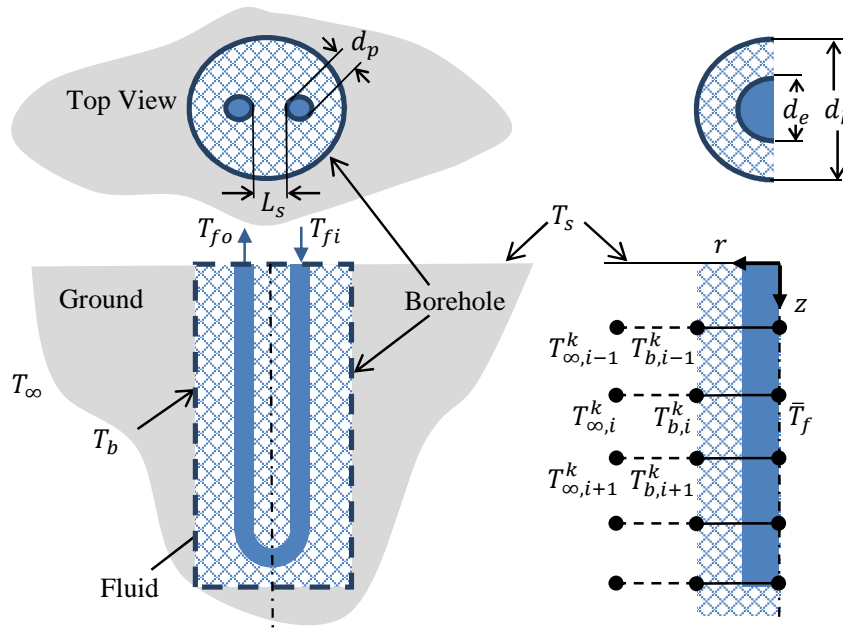
Figure 4-1.Temperature distribution of a single borehole representation (a) physical domain, (b) discretized domain along the depth (subscript of i), and time (superscript of k)

When modeling GHX using line source theory, following major assumptions are applied for each layer of the borehole,

- Phase changes of the materials in soil and the moisture migration through the borehole is neglected,

- Thermal contact resistances between the U-legs are ignored,
- Ignore the effect of ground water flow,
- Heat is transferred only through the conduction and radial direction,
- Soil thermal properties are constant,
- Neglect the end effect of the borehole.

As opposed to available models based on line source theory or cylindrical source theory, in which the heat exchange rate is considered to be constant throughout the borehole, the present study estimates the heat transfer rate at the pipe using the temperature difference between the undisturbed ground temperature, T_∞ (K) and the mean fluid temperature, $\bar{T}_f$ (K), using Equation (6).

$$q' = k_s d_e \left(T_\infty - \bar{T}_f \right) \sqrt{\pi / \alpha_s t} \qquad (6)$$

where, d_e is the equivalent diameter of a single pipe that replaces the U-legs of the pipe and calculated as follows [14]:

$$d_e = \sqrt{2 L_s d_{po}} \qquad (7)$$

where, L_s is the shank spacing between the two U-legs of the pipe, and d_{po} is the outer pipe diameter.

The existing analytical models use discontinuous heat pulses at each time step and constant along the borehole wall, which makes these models computationally expensive when targeted heat load is changing continuously in time. The use of Equation (6) brings the advantage for the developed model as it does not need to aggregate the temperature drop down at each time step and allows continuous variation of heat exchange rate with the temperature difference between the fluid and the undisturbed ground temperature. Equation (6) considers a surface of a semi-infinite solid medium with initial temperature of T_∞ which is brought into a temperature of $\bar{T}_f$, the fluid mean temperature $(T_{fi} + T_{fo})/2$ [55]. The mean fluid temperature, which is calculated as the average of the inlet and outlet temperature of GHX, can be approximated as uniform throughout the pipe length considering the temperature variation in the U-legs. To account the non-uniform distribution of the ground temperature

into heat transfer rates, the model developed by Kusuda and Achenbach [56] is used and it is given in Equation (8). This is a solution for transient heat conduction in the ground where the ground surface temperature is changing periodically. Therefore, it can handle temporal changes in the ground surface temperature as well.

$$T_\infty = \bar{T}_s - T_{\text{amp}} \exp\left(\sqrt{\pi/365\alpha_d}\right) \cos\left(\left(\frac{2\pi}{365}\right)\left(t_{year} - t_{shift}\right.\right.$$
$$\left.\left. - \frac{z}{2}\left(\sqrt{\frac{365}{\pi\alpha_d}}\right)\right)\right)$$

(8)

where, T_∞ is the undisturbed ground temperature (K), $\bar{T}_s$ is the mean surface temperature (K) which can be approximated as the average air temperature or undisturbed ground temperature at infinite depth, T_{amp} is the amplitude of surface temperature variation (K), z is the depth below the ground surface (m), α_d is the thermal diffusivity of soil (m²/day), t_{year} is the current time in days, t_{shift} is the coldest day of the year.

After substituting q' into the Equation (5), borehole wall temperature can be calculated. To evaluate the transient fluid temperature variations, internal resistances in the borehole should be considered. Therefore, effective heat transfer rate into the fluid, q'_f, can be calculated as follows,

$$q'_f = \frac{\left(T_b - \bar{T}_f\right)}{R_b}$$

(9)

where R_b is the total thermal resistances (mK/W) of the borehole and they can be calculated as follows,

$$R_b = \frac{1}{2\pi d_{pi}h} + \frac{\ln\left(\frac{d_{po}}{d_{pi}}\right)}{4\pi k_p} + \frac{\ln\left(\frac{d_b}{d_e}\right)}{2\pi k_g}$$

(10)

30

where, d_{pi} is the inner diameter of the pipe (m), d_{po} is the outer diameter of the pipe (m), d_b is the diameter of the borehole (m); k_f, k_p, k_g are the conductivities of the fluid, pipe (W/mK), and grout respectively. h is the convection coefficient of the fluid (W/m²K), and can be calculated as follows [55],

$$h = \frac{k_f}{d_{pi}} 0.023 Re^{0.8} Pr^{0.35} \tag{11}$$

where, Pr and Re are the Prandtl number and Reynolds number respectively. The total amount of heat transferred to the fluid can be calculated as follows,

$$Q = \int_0^H 2q_f' dz \tag{12}$$

where, Q is the total amount of heat transferred to the fluid (W), H is the depth of borehole and z is the integral variable. To calculate the fluid temperature, heat balance for fluid for very small period of time dt is considered.

$$\forall \rho c_{p,f} \frac{d\bar{T}_f}{dt} = \dot{m} c_{p,f} (T_{fi} - T_{fo}) + Q \tag{13}$$

where, $\forall$ is the volume of pipe with equivalent diameter to the two U-legs. ρ and $c_{p,f}$ are the density of fluid and the heat capacity of fluid (water). $\dot{m}$ is the mass flow rate. T_{fi} and T_{fo} are the inlet and outlet fluid temperature of the GHX.

To find the new outlet fluid temperature at the new time step, $k + 1$, above equation can be rearranged as follows,

$$\forall \rho c_{p,f} \frac{(T_{fi}^{k+1} + T_{fo}^{k+1}) - (T_{fi}^k + T_{fo}^k)}{2\Delta t} = \dot{m} c_{p,f} (T_{fi}^{k+1} - T_{fo}^{k+1}) + Q \tag{14}$$

From Equation (14), the outlet temperature of the GHE can be obtained as follows,

$$T_{fo}^{k+1} = \frac{\forall \rho c_{p,f} (T_{fi}^k - T_{fi}^{k+1} + T_{fo}^k) + 2\Delta t \dot{m} c_{p,f} T_{fi}^{k+1} + 2\Delta t Q / c_{p,f}}{\forall \rho c_{p,f} + 2\Delta t \dot{m} c_{p,f}} \tag{15}$$

4.2 Detailed finite volume (FV) model

In this section, a fully developed three dimensional finite volume (FV) model is developed in order to validate the proposed semi-analytical model in the section 4.1.

Development in computational fluid dynamics (CFD) has led to growth of several commercial software packages and alternative open-source programs. One of the most reliable and accurate open-source tools currently available in open-source community for CFD calculations is OpenFOAM, a set of C++ libraries that use finite volume method to simulate 3-D geometries and unstructured grids on the Linux platform [57]. It has been applied in this present work for study of heat transfer rates, borehole wall temperature and fluid temperature and validates the proposed semi-analytical model.

OpenFOAM tools fall into two categories such as solvers and utilities [58]. Solvers are consisted of set of equation for solving physical problems and utilities are for data manipulations including pre- and post-processioning [58]. According to physical characteristic of the problem, user can select a suitable solver for simulations. blockMesh and snappyHexMesh are the mesh generating utilities in OpenFOAM, where former is for generating simple meshes and later is for complex mesh generation. Pre-processing part includes creation of the mesh according to the geometry of the problem and defining the numerical schemes to solve the equations in solver utility. Post-processing utilities are for visualizing the solution (geometry and snap shots of the simulation results). OpenFOAM provides paraFoam as the post-processing utility [58].

First, based on the borehole diameter, pipe diameter, shank spacing, length of the borehole and boundary of the bore-field, an automatically adjustable three dimensional rectangular coordinate system is designed in blockMesh utility. Pipes, borehole and the rest of the numerical domain (soil) were represented with cuboids with an equivalent width corresponding to actual diameters of the same. Since bore-field is a combination of elements with different length scales, grid sizes have to be selected carefully in order to capture the temperature variations in the bore-field accurately. The outer radius of the numerical domain is selected considering the remarks of Eskilson [3] stating Fourier number based on the radius of influence is in the order of 9.

Since numerical model is developed to understand the short term temperature response of the borehole wall, distance from the borehole in both transverse and vertical direction to outer edge of the numerical domain is stetted into 5.5 m which is approximately the maximum distance that a heat wave can travel within 50 days. As temperature gradient from the pipe surface to far field is decreasing in the transverse direction, grid size should also be selected such that the mesh near the pipe is finer and gradually become coarser as it away from the pipe. Otherwise, selecting finer grid for whole bore-field can be computationally much expensive. Figure 4-2 shows the grid prepared to represent the physical domain.
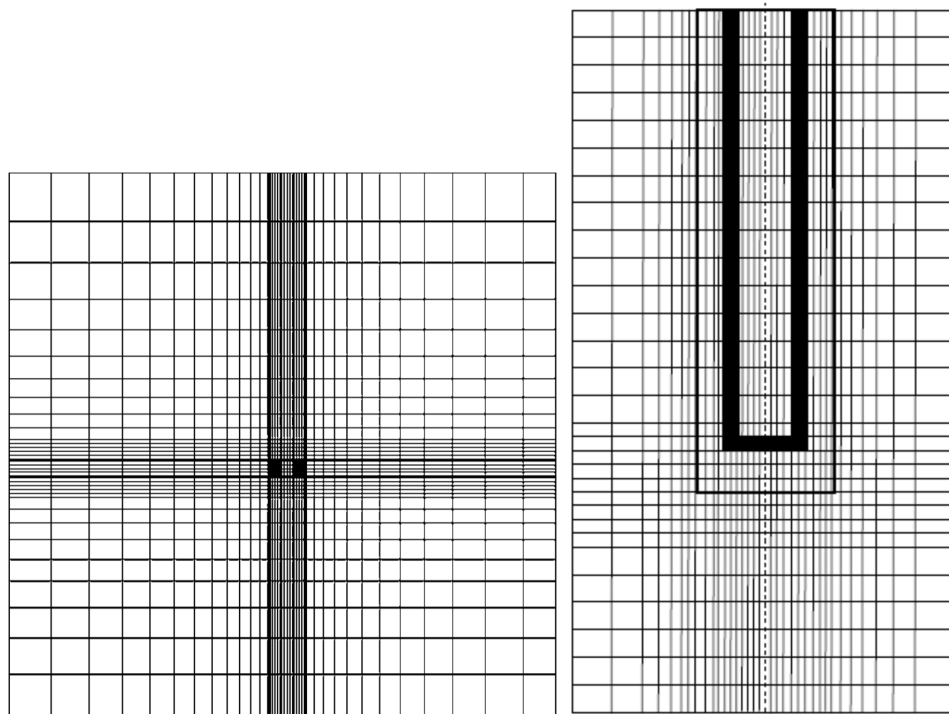
Figure 4-2. Grid used for the bore-field (a) top view, (b) side view

As pipe, borehole, soil and water are consisted with different thermo physical properties, the entire grid is divided into four regions (using utility: topoSet) namely pipe, water, and borehole and soil. Then, each of these regions were assigned with their corresponding thermo physical properties separately.

To simulate the temperature profile of the fluid (water) and solid regions (pipe, soil and borehole), solver should be selected such that it can be able to handle multiple regions. As chtMultiRegionFoam is the only available solver in OpenFOAM that can handle the multiple regions [59], this thesis use the same. It solves Laplace equation for each solid region as given in Equation (16) and Navier-Stokes equations ((Equations (17)-(18)) and energy conservation equations (Equation (19)) for fluid region separately.

$$\frac{\partial T}{\partial t} = \alpha_s \frac{\partial^2 T}{\partial x_i \partial x_i} \tag{16}$$

where, α_s is the thermal diffusivity, which takes multiple values depending on the region under consideration in the computational domain such as pipe, grout and soil.

$$\cdot \frac{\partial u_i}{\partial x_i} = 0 \tag{17}$$

$$\rho \frac{\partial u_i}{\partial t} + \rho u_j \frac{\partial u_i}{\partial x_j} = -\frac{\partial p_i}{\partial x_j} + \frac{\partial}{\partial x_j}(2\mu S_{ij}) + \rho g_i \tag{18}$$

$$\rho \frac{D}{Dt}(h + \frac{1}{2}u_i u_i) = \frac{\partial p}{\partial t} + \frac{\partial}{\partial x_i}(u_i S_{ij}) - \frac{\partial q''}{\partial x_i} + \rho g_i u_i \tag{19}$$

where u_i represents the velocity components in three dimensional coordinates (ms^{-1}), ρ is the density of the water region (kgm^{-3}), p is the pressure (kgm^{-1}s^{-2}), g is the gravitational acceleration, h is the enthalpy ($c_{pf}T_f$), q'' is the heat flux (Wm^{-2}), S_{ij} is the strain tensor ($\frac{1}{2}(\frac{\partial u_i}{\partial x_j} + \frac{\partial u_j}{\partial x_i})$, and $\frac{D}{Dt}$ represents the ($\frac{\partial}{\partial t} + u_i \frac{\partial}{\partial x_i}$) [57].

ChtMultiRegionFoam solves the corresponding equations for each region separately using their own mesh, with access to their fields, material properties, solver controls [60] and coupling is achieved through boundary condition update [61]. The assumptions used in developing the semi-analytical model are used for the CFD model development as well.

To obtain the initial condition for temperature in solid region, Equation (8) is used. For the soil region, the top boundary is set to constant ambient air temperature which is also calculated from Equation (8) for a particular day. Temperature at outer boundaries was set to the no flux

conditions. For the pipe and grout, same boundary conditions were imposed. For the water region, at the inlet, constant velocity, constant temperature, zero pressure gradient were imposed. At the outlet, zero velocity gradient, zero temperature gradient and constant pressure (uniform zero) conditions were given. At the interface between water and the pipe, no slips velocity boundary condition and zero pressure gradients were imposed. To ensure the forced convection in the water region, gravitational acceleration was set to zero. Turbulence was not modeled as the flow was assumed as laminar. The coupling between different regions is ensured at the boundaries using a FFTB method [60] (Flux Forward, Temperature Back) in which it assured that heat flux and the temperature is conserved at the interfaces as in Equations (20) and (21).

$$T_1\big|_{\partial_{1-2}} = T_2\big|_{\partial_{2-1}} \tag{20}$$

$$k_1 \frac{\partial T_1}{\partial x}\bigg|_{\partial_{1-2}} = k_2 \frac{\partial T_2}{\partial x}\bigg|_{\partial_{2-1}} \tag{21}$$

OpenFOAM uses finite volume as the discretization scheme. To calculate the properties at the cell nodes, integral form of the conservation equations are taken. To calculate the fluxes at the cell faces, interpolations between the cell nodes are taken. It uses PIMPLE algorithm which is a combination of PISO (Pressure implicit with splitting of operator) and SIMPLE (Semi-Implicit Method for Pressure-Linked Equations) to calculate the unsteady state simulations for pressure-velocity coupling in the fluid region. The algorithm and the description of the PIMPLE can be found in [59]. Discretization schemes and the interpolation scheme used for energy equation, momentum and continuity equation are given in Table 4-1.

Table 4-1.Descretization scheme

	scheme	Interpolation
Time	Implicit Euler	-
Gradient	Gauss	linear
Divergence	Gauss	linear / upwind
Laplacian	Gauss	linear limited corrected 0.333

After discretizing the equations into system of linear algebraic equations, gradients methods like PCG (Preconditioned conjugate gradients method) and PBiCG (Preconditioned bi-conjugate gradient method) are used to solve the matrices depending on their symmetric and asymmetric properties [59].

4.3 Results and discussion

4.3.1 Comparison against literature

Proposed semi-analytical model is compared with the numerical model developed by Yavuzturk and Spitler [3]. He has developed non-dimensional short time step temperature response factors (g-function curves) assuming uniform ground temperature profile and constant heat flux along the borehole wall. To compare new model with [3], it is necessary to produce non-dimensional temperature response factors for a single borehole. The g-function, as given in [3], is used for a borehole with non-dimensional radius (r_b/H) 0.0005 and for non-dimensional time ($\log(t/t_s)$) period of approximately -15 to -8 which corresponds to 2.5 minutes and 200 hours, in which t_s is the characteristic time scale ($H^2/9\alpha$); H and r_b are the depth and radius of the borehole, respectively. Accordingly, borehole radius is selected as 0.05 m and depth as 100m. Also, thermo-physical parameters and turbulent properties that used for the simulations are illustrated in Table 4-2. Undisturbed ground temperature is modeled using Equation (8). Since the curve is corresponded with non-dimensional response factor when a constant heat pulse is applied over the time period, it is required to maintain a constant Q (total heat transferred amount (W)) during the time period. This is achieved by modifying the fluid's inlet and the outlet's temperatures at each time step. The algorithm is summarized as follows,

1) Set targeted heating/cooling load, i.e. Q_{target} = 6000 W
2) Specify initial guess for the inlet fluid temperature; i.e. T^0_{fi} = 5 °C
3) Assume the initial fluid outlet temperature T^0_{fo} to be the same as the fluid inlet temperature
4) Calculate $\bar{T}_f$ taking the average of inlet and outlet temperature
5) Calculate q' at the borehole wall using Equation (6)
6) Calculated borehole wall temperature using Equation (5)
7) Calculate q'_f using Equation (9) which incorporates the borehole thermal resistances
8) Calculate Q using Equation (12)

9) Calculate the new outlet temperature T_{fo}^{k+1} using Equation (15)

10) Update inlet temperature T_{fi}^{k+1} if Q and Q_{target} are different using following equation,

$$T_{fi}^{k+1} = \frac{(Q - Q_{target})}{\dot{m}c_{p,f}} - (T_{fo}^{k} - T_{fi}^{k} - T_{fo}^{k+1})$$ (22)

Above steps are repeated for each time step during the simulation time period. Because Yavuzturk and Spitler [3] assumed a uniform ground temperature profile and constant borehole wall temperature along the borehole, the comparison is carried over a single g-function, which is defined as follows:

$$g(t/t_s, r_b/H) = \frac{2\pi k_s (\overline{T}_\infty - \overline{T}_b)}{\overline{q}'_f}$$ (23)

The simulations of the developed model are carried out (using steps 2-10) considering the variation of the heat exchange rate and the undisturbed ground temperature profiles along with the depth while they are averaged (over the depth) to obtain the average heat transferred to the fluid ($\overline{q}'_f$), the average borehole temperature ($\overline{T}_b$) and the average undisturbed ground temperature ($\overline{T}_\infty$). The comparison of g-functions are given in Figure 4-3, which shows that average temperature response of the borehole calculated by semi-analytical model shows good agreement with Yavuzturk and Spitler [3] between the time periods of 2 hours to 200 hours (non-dimensional form approximately from -13 to -8) while differences are prominent before 2 hours of simulations. This is due to the fact that the present model starts with an arbitrary inlet temperature and adapts its value according to the targeted Q. Once the fluid temperature of the present model attains an equilibrium, both results agree well with each other. The differences at the earlier stages are inevitable and it can be understood further by looking at the changes in inlet and outlet fluid temperature, and total amount of heat transferred along the borehole which are depicted in Figure 4-4.

Table 4-2 Thermo physical and turbulent properties of the borehole system

Element	Properties	Values
Soil	Density (kg/m^3)	2200
	Specific heat capacity (Jkg^{-1}K^{-1})	2420
	Thermal conductivity (W/mK)	1.45
Borehole (Grout)	Density (kg/m^3)	1500
	Specific heat capacity (Jkg^{-1}K^{-1})	800
	Thermal conductivity (W/mK)	1
Pipe	Density (kg/m^3)	1100
	Specific heat capacity (Jkg^{-1}K^{-1})	1465
	Thermal conductivity (W/mK)	0.43
Water	Density (kg/m^3)	1000
	Specific heat capacity (Jkg^{-1}K^{-1})	4182
	Thermal conductivity (W/mK)	0.56
	Viscosity (m^2/s) @ 7^{0}C	1.519x10^{-6}
	Velocity (m/s)	0.1
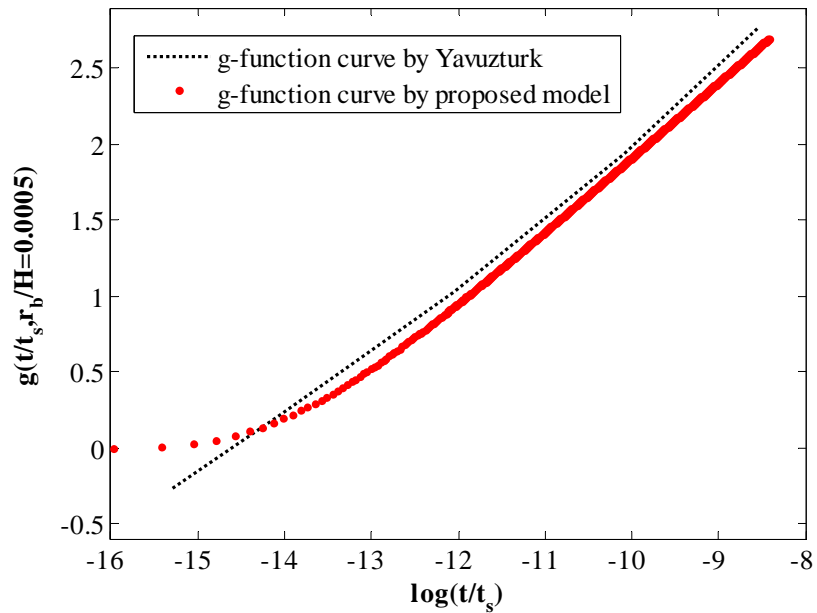
Figure 4-3.Comparison between present method and Yavuzturk and Spitler [3] for short time step g-function curves
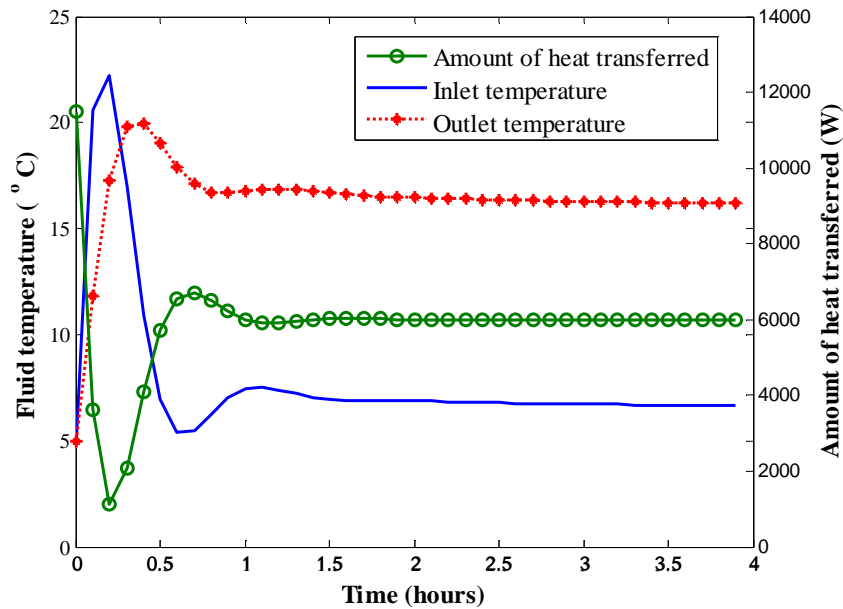
Figure 4-4. Comparison of variations in inlet fluid temperature, outlet fluid temperature and total amount of heat transferred against time.

4.3.2 Validation against finite volume (FV) model

The model is also compared to the results obtained using a detailed CFD simulation, which are conducted to calculate the short term response of the ground when ground is cooling by GHX (ground acting as a heat source). Undisturbed ground temperature profile is calculated using Equation (8) for January 1st for Northern Cyprus conditions, i.e. mean surface temperature, $\bar{T}_s$ as 22.1 ^{o}C; amplitude, A , as 21.5 ^{o}C; α_d as 0.025 m^2/day; t_{shift} as 29 (days) and t_{year} as zero. The calculated undisturbed ground temperature profile as illustrated in Figure 4-5 is used during the simulations of both semi-analytical model and for the CFD model. Thermo-physical properties as given in Table 4-2 are used for a single borehole characterized by the parameters presented in the Table 4-3.

Simulation results of semi-analytical model shows a reasonable agreement with the CFD model simulations. It can be seen that heat transfer rates are depth dependent and they are reducing with time. After almost one hour, heat transfer rates reach a quasi-steady state. Figure 4-7 shows the variation of heat transferred to fluid in depth. This is due to the fact that ground temperature distribution is not uniform along the borehole. As the first few meters of

ground below the surface temperature is less than the mean fluid temperature, heat is transferred back into the ground rather than extracting it from the ground. Therefore, heat transfer rates at the first few meters of the borehole are in the opposite direction, which illustrates that the first few meters of the borehole is not effective. Once the fluid is in the borehole where the ground temperature profile is constant (approximately after 10 m from the ground), fluid is able to extract the heat from the borehole. This emphasizes the fact that assuming a constant load along the borehole not only affects the accurate prediction of the fluid outlet temperature, but also can cause over or under estimation of the performance of the GSHP system.
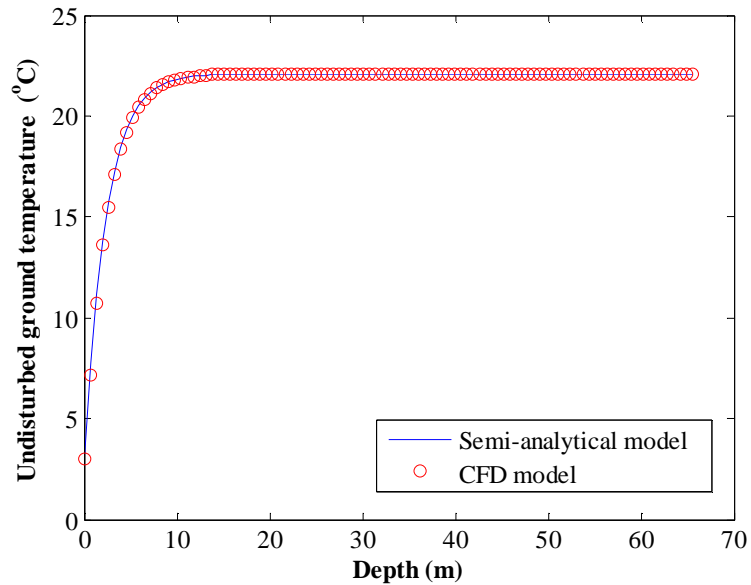
Figure 4-5. Undisturbed ground temperature variation with depth calculated using CFD model and semi-analytical model

Table 4-3 Characteristics of the borehole system

Borehole characteristics	Value
Borehole radius (m)	0.05
Borehole length (m)	60
Pipe inner radius (m)	0.013
Pipe outer radius (m)	0.016
Shank spacing (m)	0.030
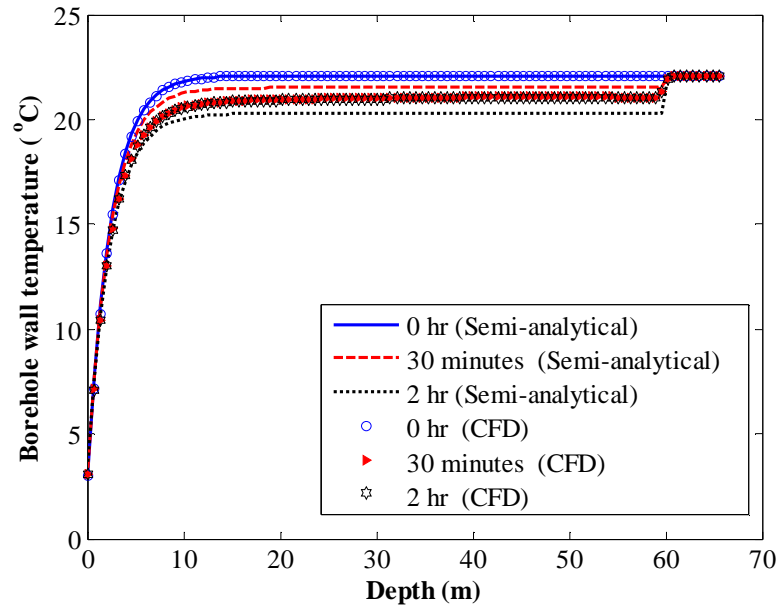
Figure 4-6. Borehole wall temperature calculated using CFD model and semi-analytical model
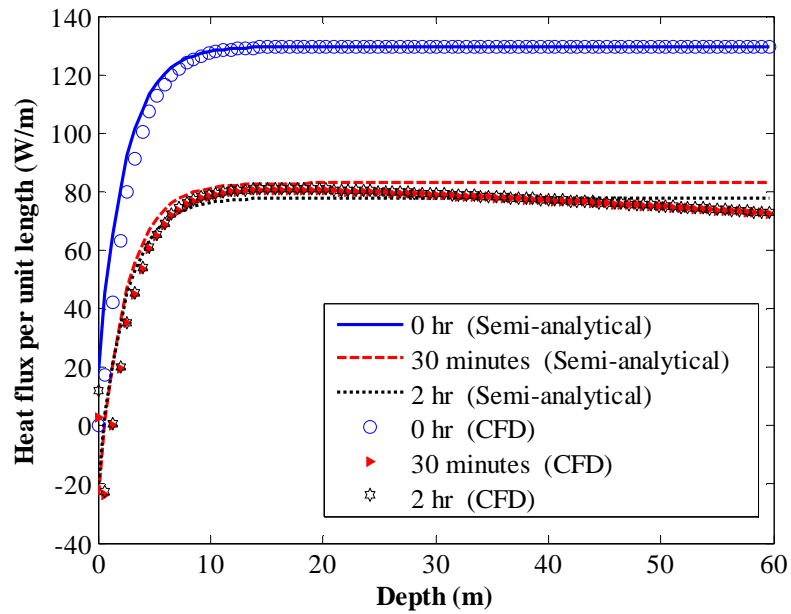
Figure 4-7. Heat flux rates into the fluid calculated using CFD model and semi-analytical model
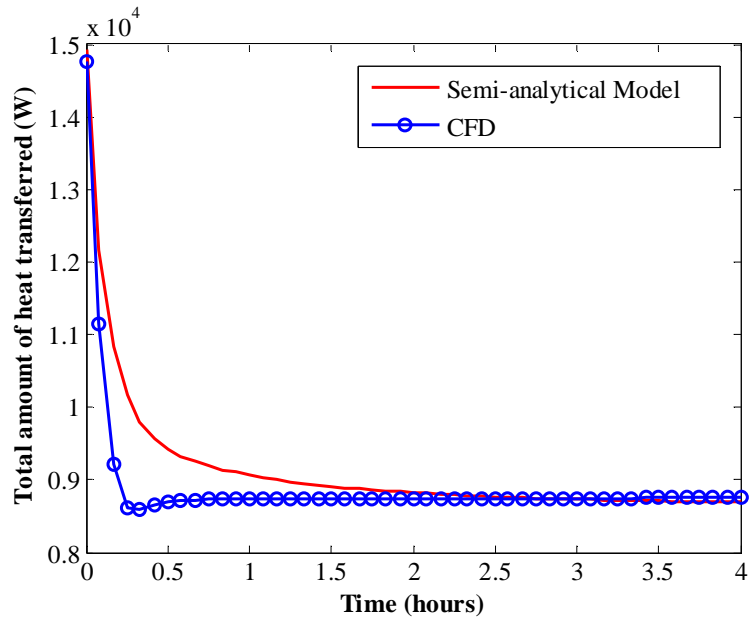
Figure 4-8. Total amount of heat transferred into the fluid calculated with CFD and semi-
analytical model
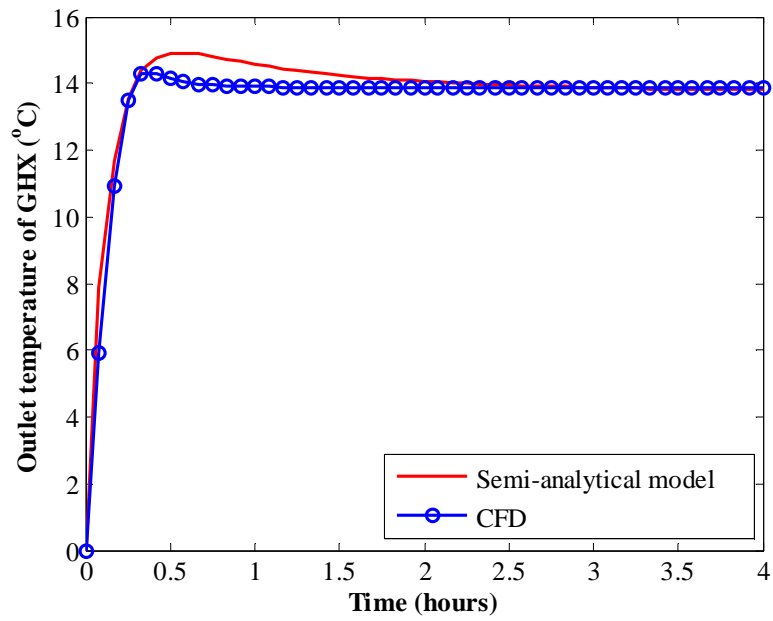
Figure 4-9. Comparison of outlet fluid temperature calculated with CFD and semi-analytical
model

Figure 4-8 shows that a large amount of heat is transferred to the fluid at the beginning of the simulation due to the temperature difference between the fluid and the ground. The heat exchange rate decays to an equilibrium condition as the field and fluid temperatures adapt.

Comparing CFD results and semi-analytical model results through Figure 4-6, it can be seen that, at the beginning, borehole wall temperature calculated from the CFD model, drops down faster than that of the semi-analytical model and reaches steady state after about 1 hour. The reason is that the semi-analytical model assumes the U-legs as a true line source rather than considering its actual geometry. In Figure 4-7, CFD results shows that heat flux per unit length increases up to some depth along the borehole and decreased whereas simulation from semi-analytical model shows that heat flux remains constant along the borehole where the undisturbed ground temperature profile is constant. The difference occurs due to neglecting the end effect of the borehole in semi-analytical model simulations.

Figure 4-10 illustrates the contour plot of temperature distribution of borehole along the total depth, cross sectional temperature distribution of borehole at 10 m below the ground surface and fluid temperature along the pipe length.
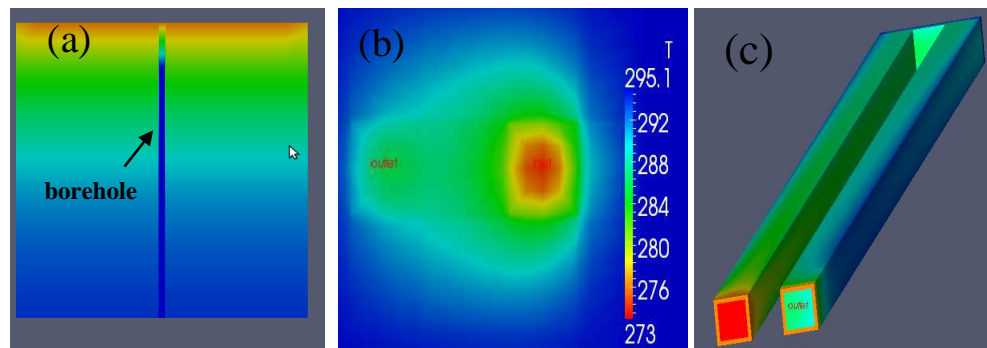
Figure 4-10. Contour of temperature distribution of element of GHX. (a) Borehole temperature distribution in the soil. (b) Borehole temperature at 10 m below the ground surface. (c) Fluid temperature distribution along the pipe

These contour plots also clearly show that undisturbed ground temperature distribution, borehole wall temperature, fluid temperatures along the pipe are non-uniform.

The simulation of ground temperature variation for 4 hour time period using three dimensional CFD model takes almost 4 hours of real time with 10 minute time steps. However, this can even be longer when magnitude of the inlet velocity is higher. Since, for stability of solutions of partial differential equations with advective terms should satisfy the CFL condition (stability condition) in which the courant number ($u\Delta t / \Delta x$) should always be less than 1(>0.5 recommended).Therefore, advantage of semi-analytical model over the three dimensional CFD model is, its ability to simulate the GHX responses for even long term periods with much smaller steps.

4.4 Summary of the chapter

In this chapter, a new semi-analytical model was developed for analyzing the short term response of the ground heat exchangers by accounting the depth dependencies in the heat transfer rates along the borehole. The novelty of the model is that it is able to predict fluid's exit temperature for both short- and long-term periods without a need to explicitly consider load aggregation at a modest computational cost. The model is validated against the existing short term ground temperature response model in the literature and a three dimensional finite volume (FV) simulations, which also address the transient behavior of the ground temperature response in sub-hourly intervals at high computational costs.

CHAPTER 5

CASE STUDY: DORM II METU NCC

This chapter presents a numerical methodology for feasibility analysis of GSHP system by integrating the semi-analytical model developed in the previous chapter with hourly heating/cooling loads of a building. A case study is conducted for dormitory II building at Middle East Technical University Northern Cyprus Campus.

Section 5.1 estimates the heating load of the dormitory II building. Section 5.2 and section 5.3 introduce GHX design model and economical optimization model to find the possible set of configuration and most economical configuration of GHX system for Dormitory II building respectively.

The semi-analytical model proposed in Chapter 4 is used in section 5.4 to develop an accurate feasibility analysis for the economically optimal configuration obtained in section 5.3.The enhanced feasibility analysis uses hourly energy consumption instead of constant ground load in order enhance the accuracy of the simulation. Section 5.5 presents results and discussion of the case study. Finally, chapter ends with a summery.

5.1 Building load estimation using OpenStudio

Building load calculation is vital when determining the GHX design parameters. In this study, open source software called OpenStudio is used to estimate the building loads. It is a collection of software including SketchUp, EnergyPlus and Radiance. SketchUp is used to model the three dimensional view of the building envelop. EnergyPlus is used for the building energy simulations. EnergyPlus required two types of input data such as weather data including basic location, latitude, longitude, time zone, elevation, peak heating and cooling design conditions and building description data such as geometry of the building, construction materials, internal load objects such as people, lights, Luminaries, electric equipment, gas equipment, steam equipment, and water use equipment, collections of schedules for building activities or elements and number of thermal zones, cooling and heating set points and HVAC equipment [62]**.**

Summary of the building cooling and heating load simulations steps can be given as follows:

1. Create 3D EnergyPlus geometry using plug in for Google SketchUp.
2. Assign the space types (E.g. Medium Office, Hospital, Secondary school, etc.) to the spaces built by SketchUp.
3. Assign the spaces into thermal zones. When building is zoned, several factors to be considered such as their usage, occupancy, activity level of occupants, exposure to the sun (interior zone, exterior zone), etc. Most buildings have more than one zone.
4. Add the location and the weather data into the OpenStudio model using EPW Weather Files
5. Modify the existing construction types (materials, thickness, and conductivity values).
6. Add HVAC equipment into each zone.
7. Modify the predefined space parameters such as temperature set points and internal loads.
8. Calculate the conduction, convection, infiltration, radiation heat gain and heat losses using the basic thermodynamic principals.

5.2 GHX design model

Designers of vertical loop ground heat exchangers need a quick methodology to estimate the length of a borehole system for a given building load. Philippe and Bernier [63] has proposed an efficient methodology to calculate the length of a borehole system considering the worst case scenario [63]. The methodology was developed using the following assumptions,

- Ground loads are constant,
- Undisturbed ground temperature is uniform
- Soil is homogeneous
- Heat transfer in the ground occurs only by conduction,
- No moisture migration,
- No underground water movements.

For a multiple borehole system, total length of a GHX system when applying constant ground loads can be given by following equation [63],

$$L = \frac{Q_{g,h}R_b + Q_{g,y}R_{10y} + Q_{g,m}R_{1m} + Q_{g,h}R_{6h}}{\overline{T}_f - (\overline{T}_s + T_p)}$$ (24)

where, L is the total length of the borehole system (m) in case of number of boreholes is more than one. $Q_{g,h}$, $Q_{g,y}$ and $Q_{g,m}$ represent peak hourly, yearly average and highest monthly heat load transfer from/to ground (W). These ground loads are positive when the heat is rejected into the ground using the GHX system (cooling the building) and they are negative when heat is absorbed from the ground (heating the building). R_{10y}, R_{1m} and R_{6h} represent effective ground thermal resistances (mKW^{-1}) corresponding to 10 years, one month, and six hours of successive heat pulses. R_b is the borehole thermal resistance (mKW^{-1}) and calculations of the same is given in Equation (10). $\overline{T}_s$ is the mean ground surface temperature (K), $\overline{T}_f$ is the mean fluid temperature (K). T_p is the temperature penalty and it is corresponded to the temperature drop down or increase at the borehole wall due to the long term interference among the boreholes in case of multiple boreholes are presented. For a single borehole, T_p is assumed to be zero. The negative penalty temperature values are corresponded with temperature drop down at the borehole and positive sign represents the increase in borehole wall temperature.

Corresponding ground loads for heating and cooling loads of a building are calculated assuming a constant *COP* of the heat pump and equation is as follows,

$$Q_{g,i} = \frac{rQ_i(COP \pm 1)}{COP}, \quad i = h, y, m$$ (25)

where, $Q_{g,i}$ represents the corresponding ground loads for heating/cooling of the building. The positive sign of the equation is taken if the loads are calculated for space cooling (ground is heated) and negative sign is corresponded with space heating (ground is cooled). Q_i is the heating/cooling load of the building (calculated using OpenStudio). r is the ratio of GSHP contribution to total heating load.

Calculations of effective thermal resistances (R_{10y}, R_{1m} and R_{6h}) are given in the Equation (26). It is an algebraic correlation to the solution originally developed using cylindrical heat source theory [64], based on large number of calculations over typical range of values for thermal diffusivity and borehole radius.

$$R = \frac{1}{k_s} f(\alpha_d, r_b) \qquad (26)$$

Where, r_b is the borehole radius (m), k_s is the thermal conductivity of the soil (W/m^{-1}K^{-1}), α_d is the thermal diffusivity of the soil (m^2/day). Function f is a simplified fitted curve to the analytical solution of the cylindrical source theory. The Equation (27) represents the formula for f-function. The correlation coefficients for f_{6h}, f_{1m} and f_{10y} corresponding to R_{6h}, R_{1m} and R_{10y} are illustrated in Table 5-1.

$$\begin{aligned} f &= a_0 + a_1 r_b + a_2 r_b^2 + a_3 \alpha_d + a_4 \alpha_d^2 + a_5 \ln(\alpha_d) + a_6 \ln(\alpha_d)^2 \\ &+ a_7 r_b \alpha_d + a_8 r_b \ln(\alpha_d) + a_9 \alpha_d \ln(\alpha_d) \end{aligned} \qquad (27)$$

However, the correlation coefficients for f-function given in Table 5-1 are valid only if the thermal diffusivity and the radius of the borehole follows the following ranges. Otherwise, the original solution of the cylindrical source theory should be developed.

$$0.05\,m \leq r_b \leq 0.1\,m$$

$$0.025\,m^2/day \leq \alpha_d \leq 0.2\,m^2/day \qquad (28)$$

Temperature penalty T_p is depended on number of boreholes (*NB*), spacing between the boreholes (*B*), non-dimensional time of operation (t/t_s), length of a single borehole (*H*) and aspect ratio (number of boreholes in longest direction over shortest direction of the bore-field). The calculation of T_p is given as follows,

$$T_p = \frac{Q_{g,y}}{2\pi k_s L} F(t/t_s, B/H, NB, A) \qquad (29)$$

where, F is a correlation function for Eskilson's [65] numerical g-functions developed in [63] by performing a linear regression analysis for 1485 cases of different parameter values for t/t_s,.*B/H*, *NB* and *A* [63]. Hence, Equation (29) is valid only if the values of the parameters of the borehole system are in the following ranges,

$$-2 \leq t/t_s \leq 3$$

$$4 \leq NB \leq 144$$

(30)

$$1 \leq A \leq 9$$

$$0.05 \leq B/H \leq 0.1$$

Therefore, when an optimization is carried out to find the best configurations which has least thermal interferences among the boreholes, some of the possible configurations can be missed. However, the methodology is much more efficient in time as there is no need to run three dimensional numerical simulations for each configuration.

Function F is calculated using Equation (31).

$$F = \sum_{i=0}^{36} b_i c_i$$

(31)

where, b and c are correlation coefficients for F and they are depicted in APPENDIX A.

For multiple borehole case, procedure of borehole length calculations are crucial as penalty temperature (T_p) for borehole system is a non-zero value. As borehole depth is required to calculate T_p which is unknown at the beginning, iterations are needed. Initially, T_p is set to zero by assuming that total heating load requirements are supplied only by a single borehole. Then, an approximate value for total length of the borehole system is found. Depending on the area for borehole installation and constraints of the model for number of boreholes, NB, B and A are loaded as the secondary inputs for T_p calculations. Depth of a single borehole (H) is calculated by dividing the total length by number of boreholes. Along with the approximated length for borehole system and secondary inputs, a new T_p value is calculated. Using the calculated new T_p value, borehole length is recalculated. The iterations are continued until a convergence is achieved and all the constraints defined at the above are satisfied.

In order to obtain the possible set of configurations for borehole system for each ratio, depth of a single borehole is calculated for all the configuration that a borehole system can have

under the area restriction and satisfying the model constraints. Figure 5-1 illustrates the overview of the GHX design model for selecting the possible all configurations for GHX system.
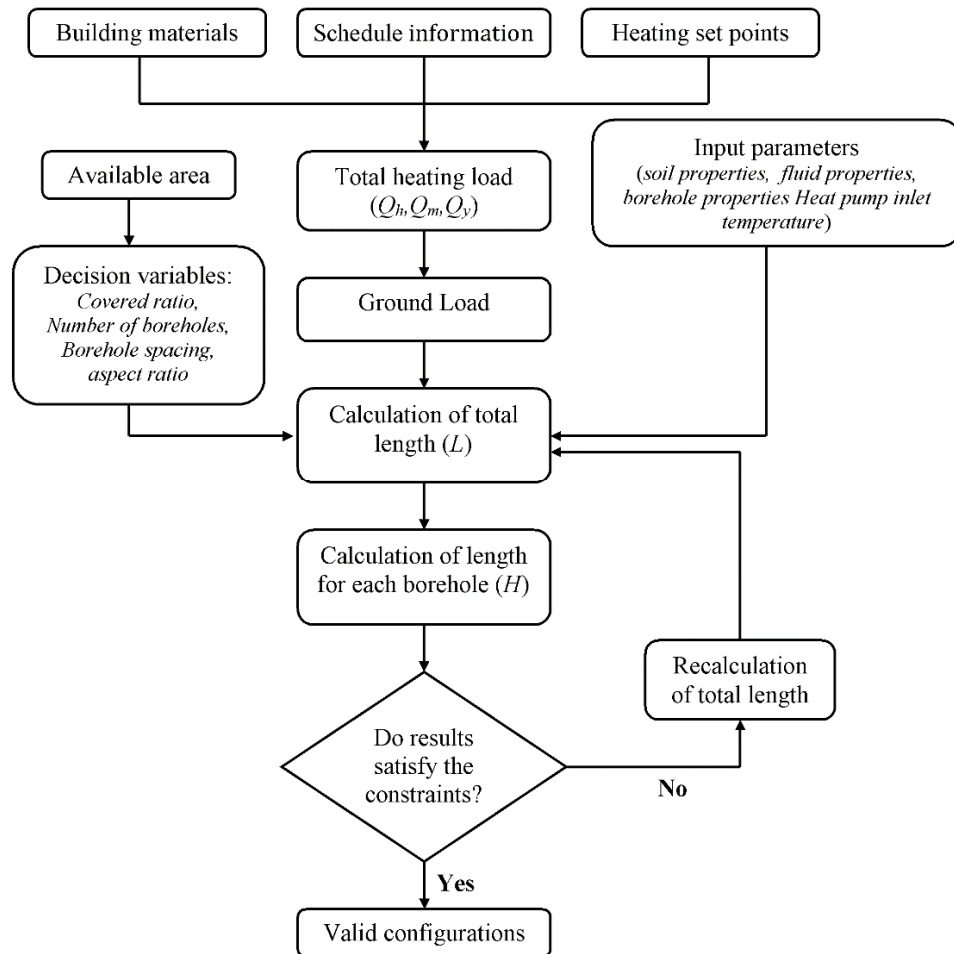
Figure 5-1 Overview of GHX design model

Table 5-1 Correlation coefficients for f_{6h}, f_{1m} and f_{10y}

	f_{6h}	f_{1m}	f_{10y}
a_0	0.6619352	0.4132728	0.3057646
a_1	-4.815693	0.2912981	0.08987446
a_2	15.03571	0.07589286	-0.09151786
a_3	-0.09879421	0.1563978	-0.03872451
a_4	0.02917889	-0.2289355	0.1690853
a_5	0.1138498	-0.004927554	-0.02881681
a_6	0.005610933	-0.002694979	-0.002886584
a_7	0.7796329	-0.6380360	-0.1723169
a_8	-0.3243880	0.2950815	0.03112034
a_9	-0.01824101	0.1493320	-0.1188438

5.3 Economical optimization model

The main objective of the optimization model is to determine the optimal configuration that has the minimum economical break-even point compared to a conventional HVAC system. Net present value (NPV) calculation is conducted. A Monte Carlo simulation are run to account the uncertainties associated with electricity prices, diesel prices, borehole installation cost and heat pump cost for NPV analysis. Finally, a break-even point analysis is carried out.

Following are the assumption that used for the NPV calculations,

- GSHP system installation cost is only consisted of borehole installation cost and heat pump installation cost
- Borehole installation cost per depth is constant along the depth
- Heating load of the building is constant in each year throughout the NPV analysis
- Maintenance cost of both boiler and the GSHP system are neglected (GSHP system has very low maintenance cost and usually it is neglected)
- Coefficient of performance (COP) of the heat pump is constant
- Thermal performance of the GSHP system is constant. i.e. no thermal depletion in the ground (The borehole system is design considering the thermal interference among the boreholes)

The Net present values (*NPV*) are calculated for varying levels of the ratios (*r*) of GSHP load contribution to total heating loads of the building over a time horizon *T*.

$$NPV_r = PVSOP_r - IC_r, \quad r = 0.1, 0.2, \ldots 1 \tag{32}$$

where, *PVSOP* is the present value of savings ($) from operating GSHP over a conventional boiler and *IC* is the total installation cost ($) of the GSHP system. *IC* includes the borehole installation cost (*BIC*) and heat pump installation cost (*HPIC*).

$$IC_r = BIC_r + HPIC_r \tag{33}$$

Borehole installation cost (*BIC*) can be calculated as follows.

$$BIC_r = NB_r \times H_r \times UBIC \tag{34}$$

where, *NB* is the number of boreholes required, *H* is the depth of each borehole (m) and *UBIC* is the borehole installation cost per unit depth ($/m).

Heat pump installation cost (*HPIC*) is mainly depended on the ground load of the GSHP system and it can be calculated as follows,

$$HPIC_r = NHPU_r \times HPUC \tag{35}$$

where, *NHPU* is the number of heat pump units required; *HPUC* is the heat pump unit cost ($/unit).

Number of heat pump units required is depended on the input power required to drive the GSHP system and the capacity of a single heat pump available in commercially. Calculation of the *NHPU* can be calculated as follows,

$$NHPU_r = \frac{(rQ_h / COP)}{1000 \times CPHPU} \tag{36}$$

where, Q_h is the peak hourly heating load of the building (W), *CPHPU* is the capacity of a heat pump unit (kW).

To calculate the present value of savings from operating GSHP system (*PVSOP*) over conventional boiler, following equation can be used,

$$PVSOP_r = \sum_{j=1}^{T} \frac{SOP_{r,j}}{(1+i_R)^j}, \ j=1,2,..T \tag{37}$$

where, *SOP* is the annual savings from operating GSHP system over a conventional boiler for space heating ($). i_R is the interest rate (%).

$$SOP_{r,j} = FCC_{r,j} - ECGSHP_{r,j} \tag{38}$$

where, *FCC* is the annual fuel consumption cost of conventional boiler ($). Usually, for the NPV calculations, operating expenditures of conventional HVAC system and the GSHP system is calculated assuming the systems run an average of 12 h per each heating degree day with the maximum heating load of the building [51], [53]. Therefore, within this section, this thesis use the same strategy for the operational cost calculations, even though the hourly energy consumption data are available.

 FCC has been included with the cost due to the difference between the heating energy consumption of the boiler with and without the GSHP system. *ECGSHP* is the annual cost for electricity consumption of GSHP system ($).

FCC is calculated as follows,

$$FCC_{r,j} = COF_j \times FCM_r \tag{39}$$

where, *COF* is the fuel cost per liter ($/L). *FCM* is the annual fuel consumption of the conventional boiler (L) and it can be calculated as follows,

$$FCM_r = \frac{(rQ_h) \times NH \times ND}{HV} \tag{40}$$

where, Q_h is the peak hourly heating load, NH is the number of operating hours of the conventional boiler (it is usually assumed 12 hours per each heating degree day) , ND is the number of days heating is required , HV is the heating value of the fuel (Wh/L).

Electricity consumption cost of GSHP system ($ECGSHP$) can be calculated by following equation,

$$ECGSHP_{r,j} = COE_j \times ECM_r \tag{41}$$

where, ECM is the electricity consumption of the GSHP system (kWh).

$$ECM_r = \frac{(rQ_h / COP) \times NH \times ND}{1000} \tag{42}$$

where, COP is the coefficient of performance of the GSHP system.

Break-even point can be calculated by finding the year that covers the total installation cost of the GSHP system by the savings from operational cost of GSHP system over conventional boiler. The following equation can be used to calculate the break-even point,

$$IC_r = \sum_{j=1}^{n} \frac{SOP_{r,j}}{(1+i_R)^j} \tag{43}$$

Where, n is the break-even point (years).

Monte-Carlo simulations are carried out to create the sample data for cost which associates with uncertainties such as electricity prices, diesel prices, heat pump cost and borehole installation cost. Electricity prices and diesel prices change yearly and fluctuate them over an average annual prices. Therefore, they are projected for next T years (Time horizon for analysis) using trend method and then, associates the uncertainties into the mean yearly prices by generating the random yearly prices over the mean by sampling from normal standard distribution since the changes in these prices are not necessarily uniform. The installation cost changes in place to place, country to country and company to company. Therefore, installation cost is also uncertain. In order to generate the uncertainties in the capital cost, uniform

distribution is used to provide a common base for comparison between different installation cost scenarios.

5.4 Enhanced feasibility analysis

In this section, semi-analytical model developed in Chapter 4 is used to conduct an improved feasibility analysis for installing the optimal configuration of GHX system obtained in section 5.3. This model utilizes the hourly variations in the heating energy consumption of building for NPV calculations to enhance the accuracy.

Hourly heating load requirements of the GSHP is achieved by modifying the fluid's inlet and the outlet's temperatures of the heat pump at each time step. In case of multiple boreholes are presented, it is assumed that all the boreholes in the GHX system supply the same amount of heat and inlet-outlet temperature of GHX are equal. Therefore, total demand of the building is distributed among each borehole equivalently.

The algorithm for calculation of hourly performance of GSHP system in space heating case is summarized as follows,

1) Specify initial guess for the inlet fluid temperature to GHX ; i.e. T_{fi}^o

2) Assume the initial fluid outlet temperature of GHX (T_{fo}^o) to be the same as the fluid inlet temperature

3) Specify initial guess for initial coefficient of performance of the heat pump; i.e. $COP^{\ 0}$

4) Calculate $\bar{T}_f$ taking the average of inlet and outlet temperature of GHX

5) Calculate q' at the borehole wall using Equation (6)

6) Calculated borehole wall temperature using Equation (5)

7) Calculate q'_f using Equation (9) which incorporates the borehole thermal resistances

8) Calculate the amount of heat transferred from ground (Q_C) to GHX using Equation (12)

9) Calculate total heating load supplied by heat pump (Q_H) using the following equation [7],

$$Q_H = \frac{Q_C}{a_1 + a_2 T_{fo}^{\ k} + a_3 T_{fo}^{\ k^2}} \qquad (44)$$

Where, a_1, a_2 and a_3 are the curve fitted coefficient of performance of heat pump determined by manufacture's catalogue data [7] .

10) Calculate required work net W_e to drive the heat pump as follows,

$$W_e = Q_H - Q_C \qquad (45)$$

11) Update the coefficient of performance COP^{k+1} as follows,

$$COP^{k+1} = \frac{Q_H}{W_e} \qquad (46)$$

12) Calculate new outlet temperature T_{fo}^{k+1} using Equation (15)

13) Update the amount of heat transferred to ground Q_C^{k+1} if Q_H and Q_{Demand} are different using the following equation,

$$Q_C^{\ k+1} = \frac{Q_{Demand}(COP^{k+1} - 1)}{COP^{k+1}} \qquad (47)$$

where, Q_{Demand} is the hourly heating load of a building (W). In case of multiple boreholes are presented, Q_{Demand} can be calculated by dividing the total heating load by number of boreholes. Also, if GSHP system contributes only a percentage of the total load of the building, then it should be multiplied by the ratio as well.

14) Update new inlet temperature of GHX T_{fi}^{k+1} if Q_H and Q_{Demand} are different (as in the case of Equation (47)) using following equation,

$$T_{fi}^{k+1} = \frac{(Q_C - Q_C^{\ k+1})}{\dot{m} c_{p,f}} - (T_{fo}^{k} - T_{fi}^{k} - T_{fo}^{k+1}) \qquad (48)$$

Above steps are repeated for each time step during the simulation time period.

NPV for installing the optimal configuration of GHX system for building is calculated using Equation (32). The ratio r and configuration of the borehole system is selected according to the optimal configurations found in Section 5.3. GSHP installation cost can be calculated using the Equations (33)-(36). The present value of savings from operational cost of GSHP system over conventional HVAC system is calculated as same as in the Section 5.3 using Equation (37). However, savings from operational cost of GSHP system over conventional boiler is now changed annually, not only due to the changes in the annual diesel and electricity price, but also due to changes in the electricity consumption and amount of energy supplied by GSHP system due to hourly/sub hourly changes in the fluid's inlet and outlet temperature of GHX.

 Annual saving from operational cost of GSHP system over conventional boiler (*SOP*) is calculated using the following equation,

$$SOP_{r,j} = FCCWT_j - (FCC_{r,j} + ECGSHP_{r,j}) \qquad (49)$$

where, *FCCWT* is the annual fuel cost of conventional boiler ($) without a GSHP system. *FCC* is the operational cost of conventional boiler in the presence of GSHP system. This includes the remaining share of the total load that should be supplied by the conventional boiler.

It is assumed that hourly or sub hourly heating loads of the building is constant in each year during the time period of analysis. *FCCWT* can be calculated as follows,

$$FCCWT_j = COF_j \times FCMWT \qquad (50)$$

where, *FCMWT* is the annual fuel consumption of the conventional boiler (L/yr) in the absence of GSHP system and it can be calculated as follows ,

$$FCMWT = \frac{\sum_{i=1}^{8760 \times \Delta t} Q_{total,\, i} \times \Delta t}{HV} \qquad (51)$$

where, Q_{total} is the total hourly/sub hourly heating demand of the building (W). Δt is the time step used in building load estimation model in Section 5.1.

FCC can be calculated as follows,

$$FCC_j = COF_j \times FCM_j \tag{52}$$

where, *FCM* is the annual fuel consumption of the conventional boiler (L/yr) in the presence of GSHP system and it can be calculated as follows ,

$$FCM_j = \frac{\sum_{i=1}^{8760 \times \Delta t}(Q_{total,i} - (Q_{H,i} \times NB)) \times \Delta t}{HV} \tag{53}$$

where, Q_H is the hourly/sub hourly heating load, supplied by GHX and *NB* is the number of boreholes in the GHX system in case of multiple boreholes are presented.

Electricity consumption cost of GSHP system (*ECGSHP*) can be calculated as same as in the previous model using Equation (41). However, annual electricity consumption of the GSHP system is calculated in a different manner than the previous model and calculation is given in the following equation,

$$ECM_j = \frac{\sum_{i=1}^{8760 \times \Delta t}(W_{e,i} \times NB) \times \Delta t}{1000}, j = 1,2,...T \tag{54}$$

where, *ECM* is the annual electricity consumption of the GSHP system (kWh/yr) and $W_{e,i}$ is the hourly/sub hourly power consumption of the heat pump (W).

Break-even point can be calculated using Equation (43).

5.5 Results and discussion
5.5.1 Building load estimation using OpenStudio

The building load estimation model developed using OpenStudio software has been implemented in a case study for a campus dormitory building located in Middle East

Technical University, Northern Cyprus Campus, Kalkanli, Guzelyurt area. Dormitory II building is consisted of two five story buildings namely block A and block B. The total floor area of the Dormitory II building is 15,748 m^2 and it is occupied by approximately 600 students (both Block A and B). Block A is a building with a flat roof consisted with Garden floor, boiler room, small laundry, canteen and student rooms while block B is consisted only with students rooms. To heat the building in winter, a non-condensing Meksis (brand) Diesel boiler with a capacity of 1,000,000 kcal/h is used. Cooling requirement is satisfied by electrically driven two air-cooled chillers of McQuary brand. Due to the complexity of the schedules and the category of the spaces in the block A, energy consumption of the HVAC system of block B was analyzed. As the students are on summer vacation, dormitory II, block B building is unoccupied during the months of June-September. Therefore, calculation of cooling load is not required. Input parameters for the building load calculation model for the block B building are presented in Table 5-2. The three dimensional view of the block B building modelled using OpenStudio software is illustrated in Figure 5-2. Table 5-3 shows the simulated peak hourly, peak monthly and yearly average heating load for the dormitory II block B building. Figure 5-3 shows the hourly variations in the heating load of the dormitory II, block B building within a one year period. The results show that peak hourly heating load is occurred in a day on February while the peak monthly heating load is happened on January.

Since, there is no breakdown of the heating energy consumption for block B and block A in the utility bills, simulated boiler's energy consumption for heating of the block B is multiplied simply by two and compared it with utility bill data for the total heating energy consumption of the dormitory II building and it is illustrated in Figure 5-4. According to the dormitory II utility bill data, boiler's total energy consumption for heating was 946,360 kWh in 2011.

The simulated results for heating energy consumption of block B is 332,042 kWh. There are several reasons for simulated results and the utility bills are differed to each other. This can be mostly due to the fact that, Block A is consisted with many energy consuming spaces than block B such as a cafeteria, boiler room and laundry room and many more opening spaces. Therefore, energy consumption of the block A should be obviously higher than that of the block B and we cannot simply compare the twice of the heating energy consumption of block B with the available data.

Also it is difficult to predict the actual energy consumption of the dormitory II since some of the building materials were unable to find in the OpenStudio library. This can also lead to deviation from the actual values from the projected values.
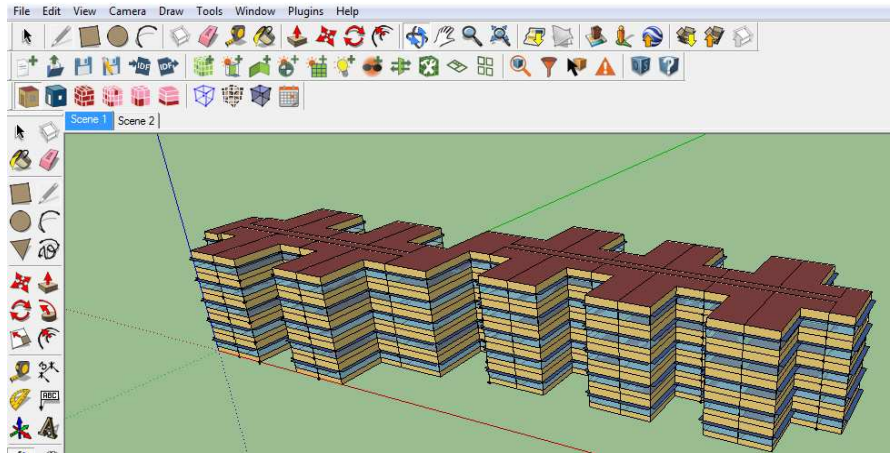
Figure 5-2 Modeled 3D view of dormitory building using SketchUp

Table 5-2 Input parameters for building load estimation

Parameters	Values or Source
Geometry	AutoCad plan
weather data	EnergyPlus Weather Files
Number of students	300
Materials	similar to block B
Total floor area (m^2)	7681
Number of thermal zones	5
Heating Set point Temperature (^{o}C)	22.1

Table 5-3 Simulated heating load for dormitory II, block B building

Heating load	value (W)
peak hourly ground load	268,900
monthly ground load	104,110
yearly average ground load	4,212
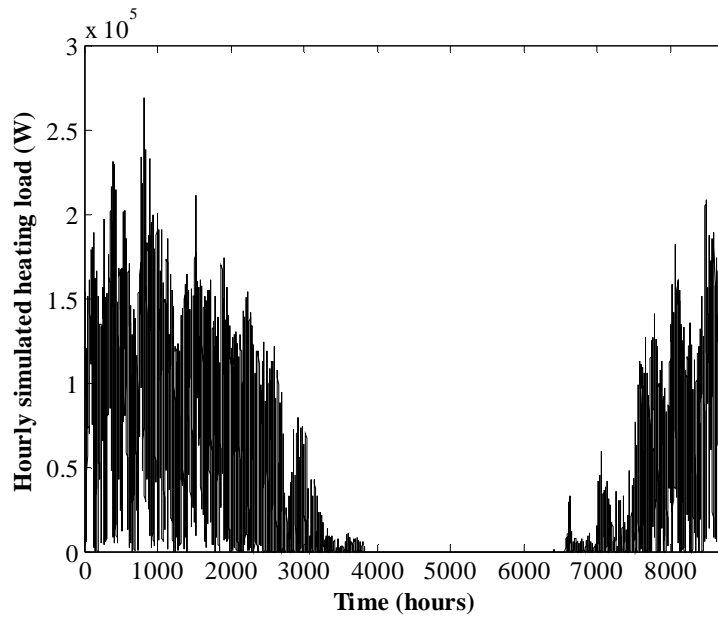
Figure 5-3 Hourly simulated heating load of dormitory II, block B building
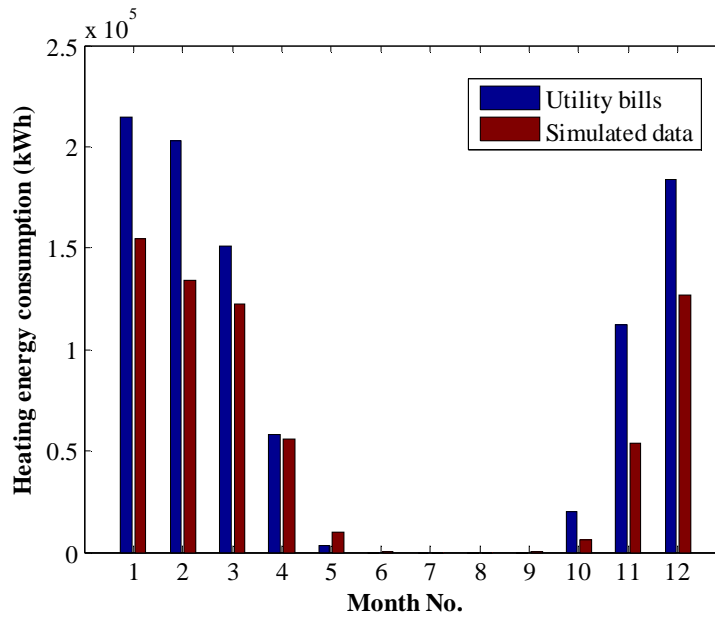
Figure 5-4 Comparison of heating energy consumption of boiler using utility bills and simulated results

Also, weather data required by EnergyPlus software to simulate the energy consumption is only available for the Larnaka, not for Guzelyurt. Furthermore, windows were unable to place at exactly the right place of the building due to its complexities. Schedules of the buildings cannot be known exactly. These all kind of missing data, make simulated results deviation from the actual energy consumption of the building. However, simulated results are qualitatively coincided with the utility bills of the dormitory II building.

5.5.2 GHX design model

First, a maximum area for installation of the boreholes was selected. The area was selected such that distance from the building to the boreholes will be the least. This will cause less piping and hence lower cost. The length and width of the selected rectangular area is 70 m and 14 m respectively. Heating loads calculated using the building load estimation model was taken as the preliminary input. Thermo-physical properties and the characteristic of the borehole system is selected as same as values use in the Chapter 4 (Table 4-2 and Table 4-3) except the length of the boreholes as it is an unknown priori at the beginning of the calculations.

Undisturbed mean ground surface temperature is taken as 22.1°C by averaging the 10 years of metrological data for surface temperature in Kalkanli, Guzelyurt area. According to the ASHRAE guidelines, entering water temperature to the heat pump should be less than the [5,10] °C from the undisturbed ground temperature [66]. Therefore, entering water temperature to the heat pump was taken as 14.5°C.

When designing a borehole system, designer has the decision leadership whether to build the borehole system either with the least deterioration over the time or with least installation cost. Equation (24) considers the worst case scenario [63] for borehole sizing and therefore over estimates the length of the borehole system. As this thesis is interested to have minimum break-even point for the GSHP system installation compared to the existing conventional boiler, all the length calculation for borehole system are conducted based on the highest monthly load together with the corresponding resistance rather than considering three successive thermal pulses that described in the Equation (24).

In order to find the least cost configuration of the borehole system for each ratio, all possible configurations that can have under the selected area for borehole installation were studied. However, the analysis was bounded by the model constraints defined in the Equation (30). Configurations includes only the spacing between the boreholes, number of boreholes and aspect ratio. The length is calculated for each ratio with aforesaid all possible configurations using Equation (24)-(29). For each ratio, 199 possible configurations were studied totaling to 1990. The space between the boreholes were restricted only to 3 m-6 m considering to have less thermal interaction among the boreholes and limitation of the area for the borehole installation.

It was found that, when adding the boreholes into the longest direction in the area by removing them in the shorter direction while keeping the total number of boreholes constant, drop down in the borehole wall temperature compared to that of previous configurations is reduced. Hence it leads to a shorter total length in the borehole system. This phenomena is illustrated in Table 5-4 when the GSHP contribution to the total heating load is only 60%. N_x and N_y are the number of boreholes in longest direction (considered as x-direction) and shortest direction (considered as y-direction) respectively.

Also, as the number of boreholes increased in the longer direction while keeping the number of boreholes in the other direction constant, temperature drop at the boreholes and the total length of the borehole system were increased. Therefore, for each ratio of the ground load, finding the best configuration that leads to decrease in the temperature drop should be found. The Figure 5-5 shows that, how the penalty temperature effect the total length of the borehole system when the GSHP contribution to the total heating load is only 20%.

The least cost configuration for each ratio was found by analyzing the configuration that gives the least value for the product of the number of boreholes into the depth of the borehole. Table 5-5 depicts the simulated result for the least cost configurations for each ratio. It can be seen that as the ratio (GSHP contribution into total heating load) increases up to 0.6, the depth of each borehole is increased. However, after 0.6 ratio, increasing the depth of the borehole for each ratio further is not possible as recommended borehole depth range is 40 m- 150 m [19]. Therefore, after 0.6 ratio, number of boreholes for each ratio was increased rather than increasing the depth of the borehole. Increasing the number of boreholes can enhance the heat transfer from ground to building as total length of the borehole system is increased as well.

Table 5-4 Penalty temperature for different configuration of the borehole system (0.6 ratio)

r	B	NB	N_x	N_y	A	H	T_p	L
0.6	3	24	12	2	6.00	48.12	-1.23	1,154.96
0.6	3	24	8	3	2.67	53.60	-2.22	1,286.89
0.6	3	24	6	4	1.50	54.05	-2.29	1,297.75

Also, it was noticed that if the ground temperature is less than that of the Cyprus like 10 ^{o}C (approximately near to the ground temperature in Japan [6]), required length for the same number of boreholes with the same configuration as given in the Table 5-5 will be significantly longer (Figure 5-6). Further, analysis was carried out to find the borehole depth for the same configurations when the thermal diffusivity is higher than that of the Cyprus. It was found that thermal diffusivity significantly affect the total length of the borehole system (Figure 5-7) and soil with higher thermal diffusivities will have higher length for borehole system.

Table 5-5 The least cost configuration for borehole system for each ratio

r	B	NB	N_x	N_y	A	H	L
0.1	3	4	4	1	4	58.87	235.48
0.2	6	4	2	2	1	108.28	433.11
0.3	6	6	6	1	6	101.79	610.75
0.4	6	7	7	1	7	109.41	765.86
0.5	6	8	8	1	8	113.35	906.78
0.6	6	9	9	1	9	114.90	1,034.14
0.7	4	26	13	2	6.5	44.21	1,149.40
0.8	3	28	14	2	7	44.62	1,249.36
0.9	3	28	14	2	7	48.23	1,350.45
1	3	28	14	2	7	51.47	1,441.15
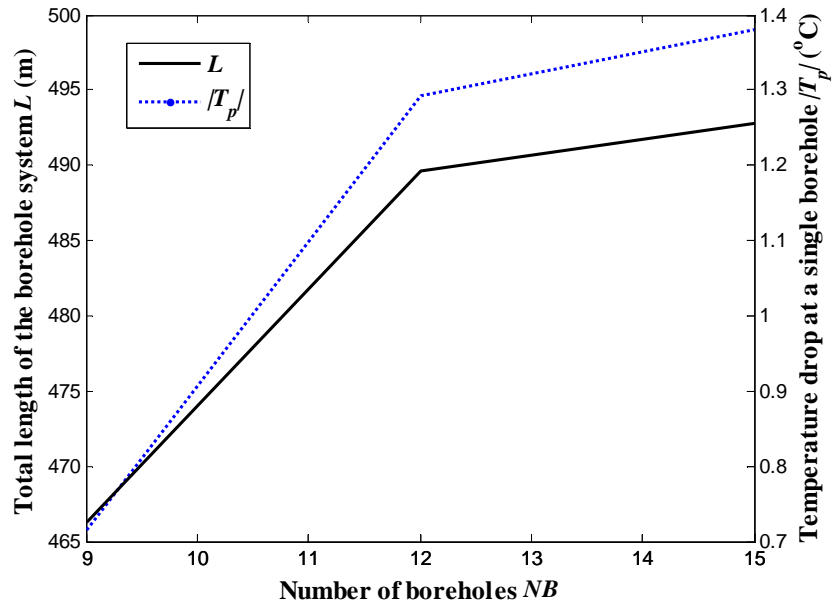
Figure 5-5 Total borehole length and temperature penalty for different number of boreholes

when $r = 0.2$
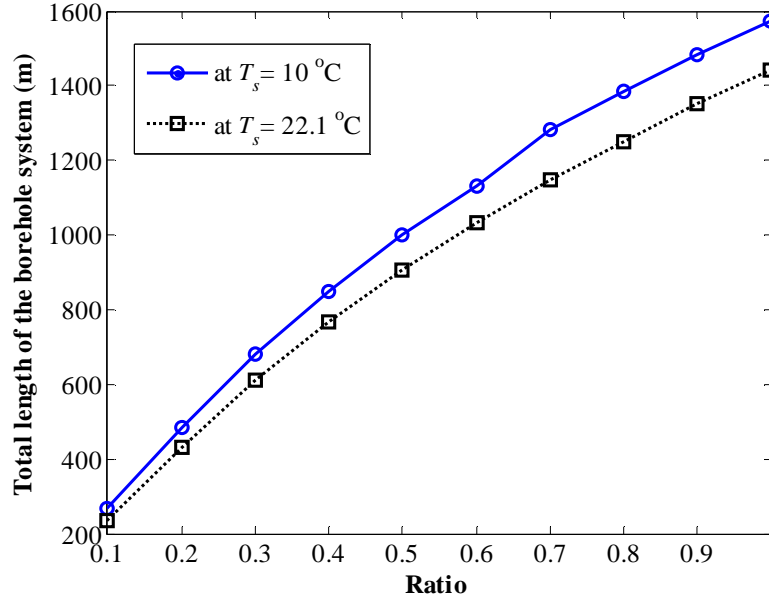
Figure 5-6 Borehole depth of the best configuration of GSHP system at each ratio for two

different ground temperatures
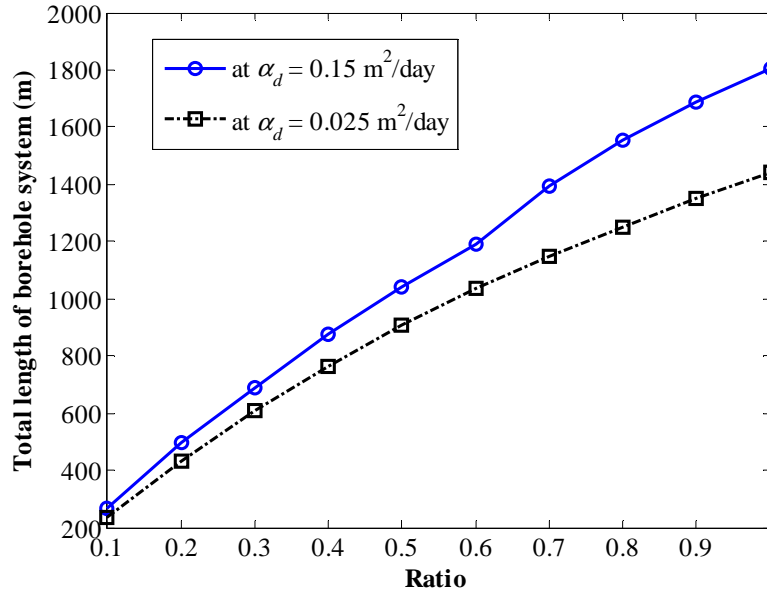
Figure 5-7 Borehole depth of the best configuration of GSHP system at each ratio for two different thermal diffusivity values of soil

5.5.3 Economical optimization model

The least cost configuration of the borehole system for each ratio was taken as the input into the optimization model. To calculate the GSHP installation cost and savings from operational cost, several cost parameters were needed. The minimum and maximum values for unit cost of these parameters are depicted in Table 5-6.

The Sources that used to obtain the values for cost parameters are listed in Table 5-6. Besides the parameters listed in the Table 5-6, electricity cost and diesel prices for next 10 year period is also required. A regression analysis was conducted to find the trend of electricity and diesel prices increases over the past 10 years and forecasted the same for the next 10 year period accordingly.

Monte Carlo simulations were carried out to generate 2000 samples for each cost parameter set in order to account the uncertainty in the cost values for installation cost, electricity and diesel prices. Figure 5-8 and Figure 5-9 illustrated the diesel and unit cost of electricity in

Cyprus for year 2015 and 2024 respectively. To calculate the heat pump installation cost and the electricity consumption of the GSHP system, COP value was assumed as 4.

Table 5-6. The minimum and maximum values for GSHP installation cost

Parameters	Min ($)	Max ($)	Source
Borehole Installation cost per unit length	43	86	[47]
Heat pump Installation cost per 10 kW	1000	8000	[67]

Present value of savings from operational cost of GSHP system and break-even point calculations were carried out by assuming 12% interest rate. Mean simulated NPV and GSHP installation cost for each ratio for the least cost configuration of the borehole system are shown in Figure 5-10. It can be seen that as the ratio increases, mean GSHP installation cost and mean net present value is also increased. As the ratio increases, total length of the borehole system should be increased, in order to supply the increasing demand. When contribution from the GSHP increases (ratio increases), operational cost is also decreased as the usage of conventional energy from the boiler is deduced. Therefore, savings from the operational cost from GSHP system is increased. The break-even points were calculated considering the mean value of the simulated GSHP installation cost and savings from operational cost of the GSHP compared to conventional boiler in dormitory II building and they are illustrated in Figure 5-11. It can be seen that within the 10 year economic life time, GSHP system with all different ratios covers the capital installation cost and the ratio which has the least break-even point is 1 and it is occurred approximately 2 years after the GSHP system installation. This illustrated that when GSHP system are installed for larger buildings with higher heating requirements, it is economically feasible to install full sized GSHP system (r=1).
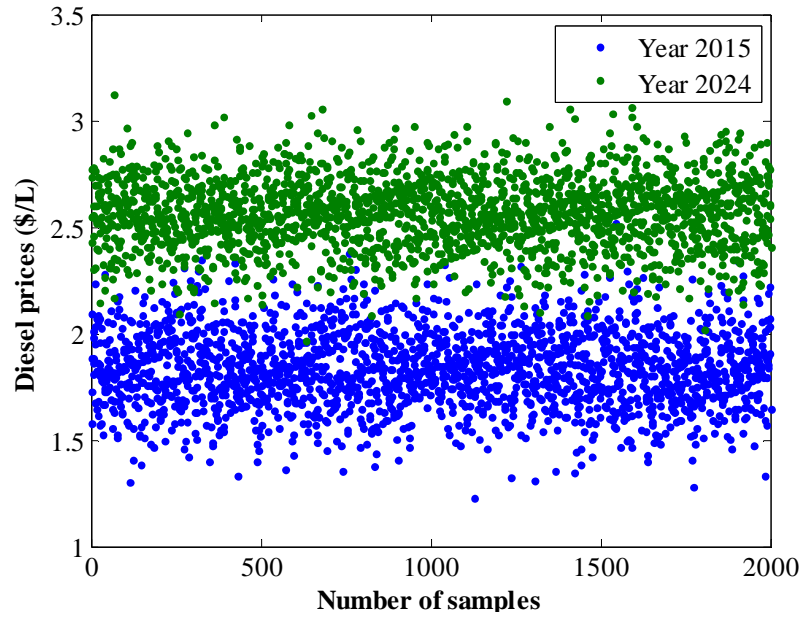
Figure 5-8 Simulated diesel prices using Monte-Carlo simulations
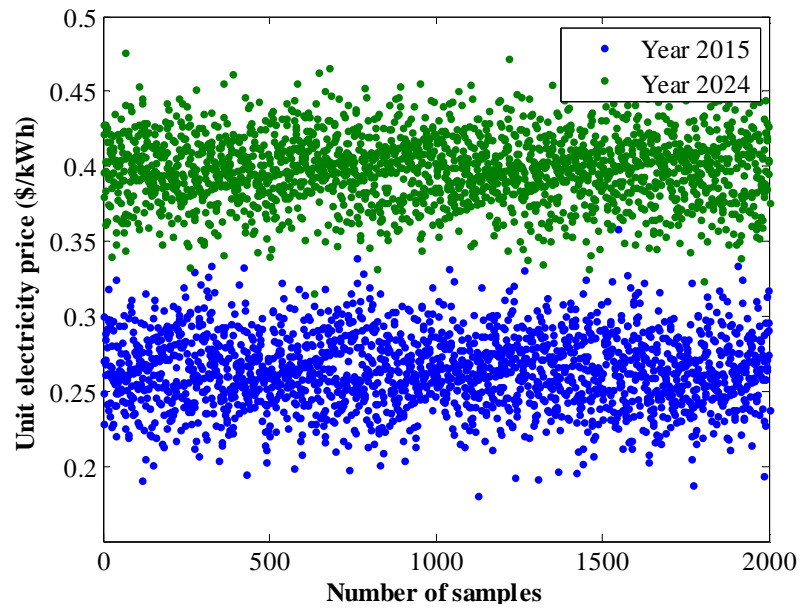
Figure 5-9 Simulated unit electricity prices using Monte-Carlo simulations
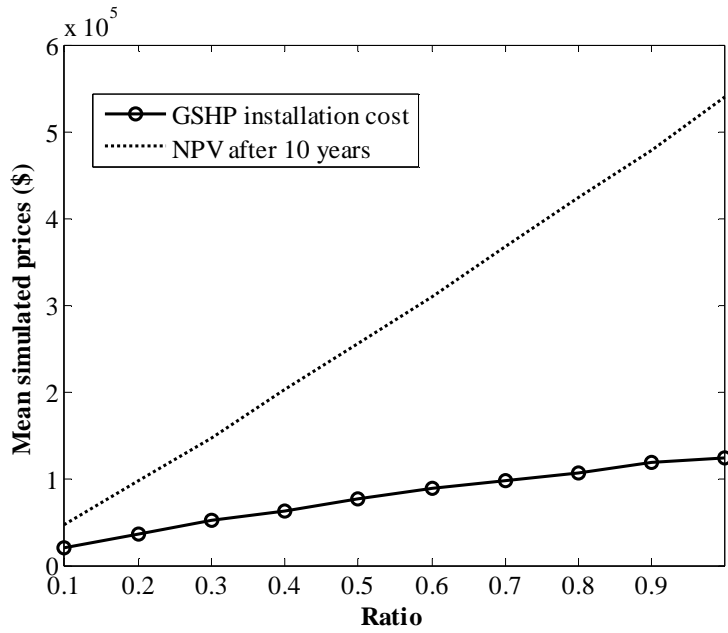
Figure 5-10 Mean simulated prices for GSHP installation and NPV after 10 years
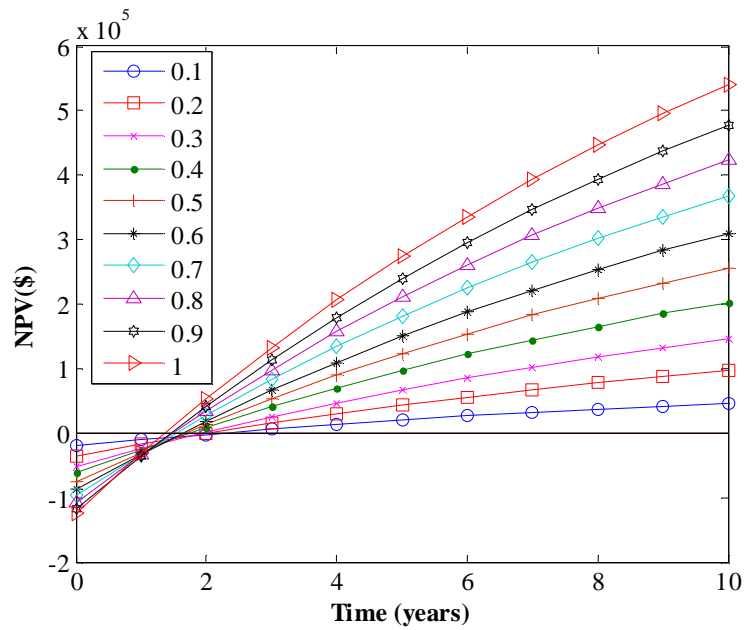
Figure 5-11 Break-even point calculations

5.5.4 Enhanced feasibility analysis

Optimal ratio that has the least break-even point is selected for the hourly performance analysis of the hypothetical GSHP system for dormitory II building. The optimal configuration of GHX system is the full sized GSHP system (r=1), consisted of 28 boreholes (14 x 2) each with 51.47 m depth and 3 m apart. The performance analysis is conducted for a single borehole in the GHX system as it is assumed that total ground load is equivalently distributed among all the boreholes. Borehole characteristic and the thermo-physical properties for the GSHP system are the same as in the GHX design model. Undisturbed ground temperature for the simulations is calculated using Equation (8). However, as the analysis is conducted to understand the hourly (or sub hourly) performance of the GSHP system, Equation (8) is also adapted to generate hourly (or sub hourly) changes in the undisturbed ground temperature as well.

Power requirements of the GSHP system during a sample day simulations are illustrated in Figure 5-12. It can be observed that heating load demand is mostly matched with the heat pump as the heat transferred to the space follows closely the demand curve. However, as seen during the adaptation periods, the model allows the heat transferred to the space, Q_H, to be over and under the demand curve. Specifically during the times where demand is higher than the supplied heat rate, a backup unit should be used to fully match the demand in this simplified GSHP system.

Figure 5-13 reveals the variation of heat transfer fluid's inlet and exit temperatures, which is captured intrinsically during the 24 hour period for the case presented in Figure 5-12, where no additional load aggregation model is imposed.

In order to study the long term behavior of the GSHP system performance, annual heating demand of the building is assumed to be constant over a 10 year period of time. Weekly average power requirements of the GSHP system within 10 year period are illustrated in Figure 5-14. Similarly adaptation in the fluids' inlet and outlet temperature to supply the required heating loads are depicted in Figure 5-15.
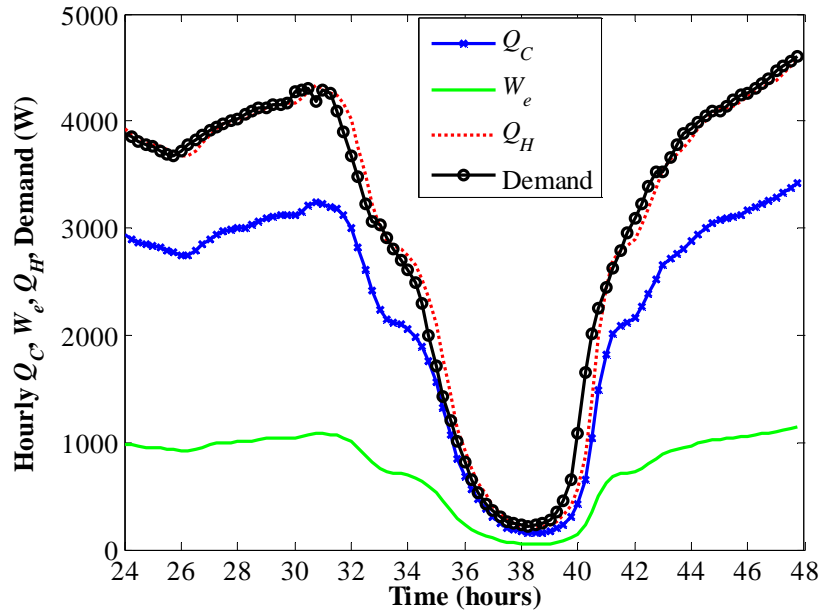
Figure 5-12 Daily simulation of a GSHP system based on the demand profile for space
heating application
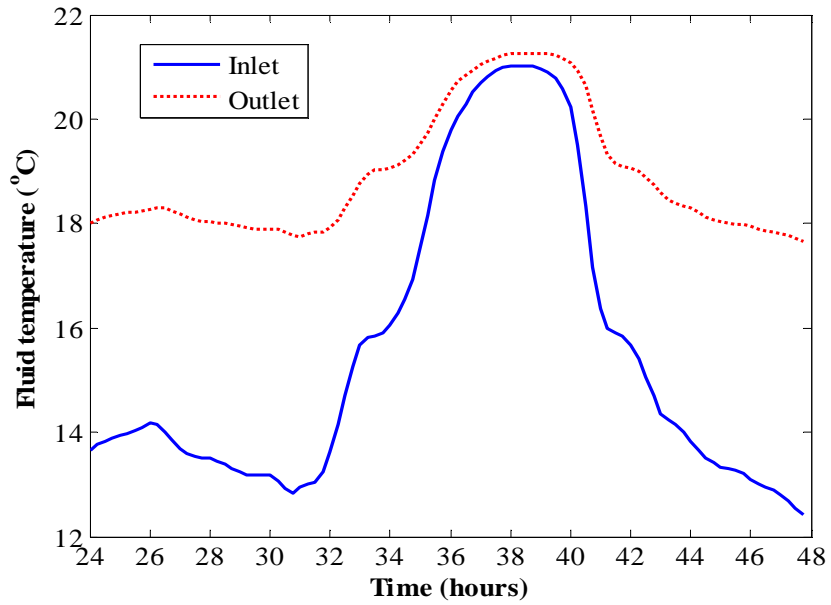
Figure 5-13 Heat transfer fluid's inlet and exit temperatures during the course of a sample
day
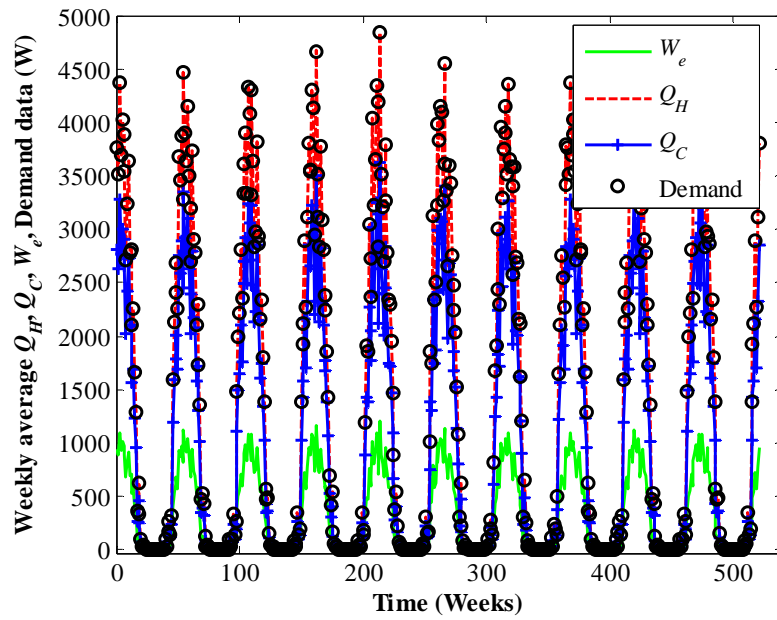
Figure 5-14 Weekly average simulation of a GSHP system based on the demand profile for space heating application for 10 year period
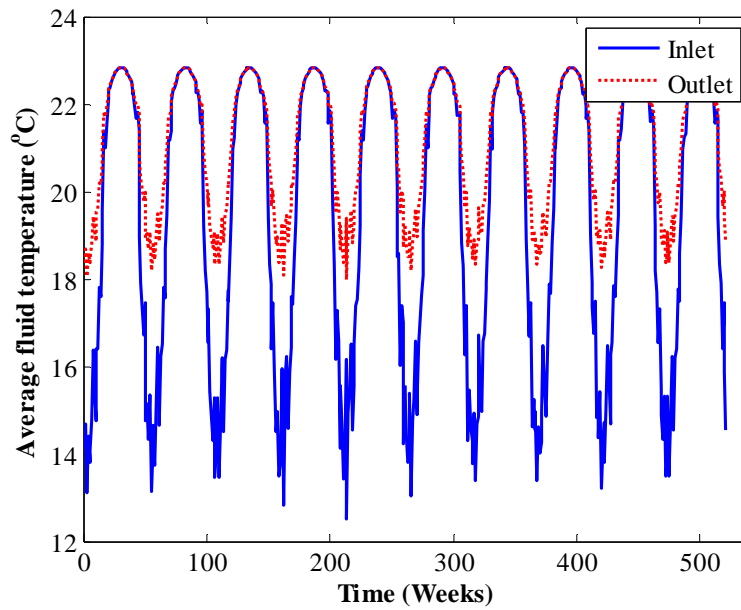
Figure 5-15 Weekly average heat transfer fluid's inlet and exit temperatures during the 10 year period

Enhanced feasibility analysis is carried out by using the method described in Section 5.4. NPV calculations were conducted for 10 year period and assumed that total heating energy consumption of the dormitory II, block B building is constant over a 10 year period of analysis. All the analysis is conducted for the same configurations of the GHX system choose in the Section 5.5.3 for optimal configuration case. Total energy absorbed from the ground, electricity consumption of GSHP system and total energy supplied by the GSHP system were simulated for 10 year period. Figure 5-17 illustrates the total heating energy consumption of building and break-down of GSHP system energy utilization over 10 year period. Table 5-7 illustrates the closer view of the simulated total heating energy consumption, total amount of energy absorbed from the ground, total amount of energy supplied by the GSHP system and total electricity consumption of the GSHP system over the 10 year period of analysis of the dormitory II, block B building.

Figure 5-17 shows the variations in the amount of energy that can extracted from the ground over the 10 year period. It is clear that, over the 10 years of time period, the GHX capability for supplying the demand of the building is reduced slightly. Therefore, in order to supply the required heating load of the building, work net need to drive the GSHP system should be increased. Figure 5-18 depicts the electricity consumption of the GSHP system over the 10 year period of analysis. It shows that, electricity consumption of the GSHP system has increased over the time.

After simulating the electricity consumption of GSHP system over 10 year period with 15 minute time step, it has been used to calculate the break-even point of GHSP system against the conventional boiler in the dormitory building for space heating application. As in the Section 5.5.3, uncertainty in the cost parameters were accounted into the NPV calculations by running the Monte-Carlo simulations. Figure 5-19 depicts the simulated data for savings from operational cost of GSHP system (SOP) over 10 year period, net present value for 10 years (NPV) and GSHP installation cost. Finally, between break-even point calculated from the economical optimization model and the enhanced feasibility analysis were compared and it is illustrated in Figure 5-20. It can be seen that, break-even occurs approximately 4 years after installing the GSHP system in dormitory II building area when using the method described in Section 5.4. However, it is almost 2 years after the one calculated at the Section 5.5.3.
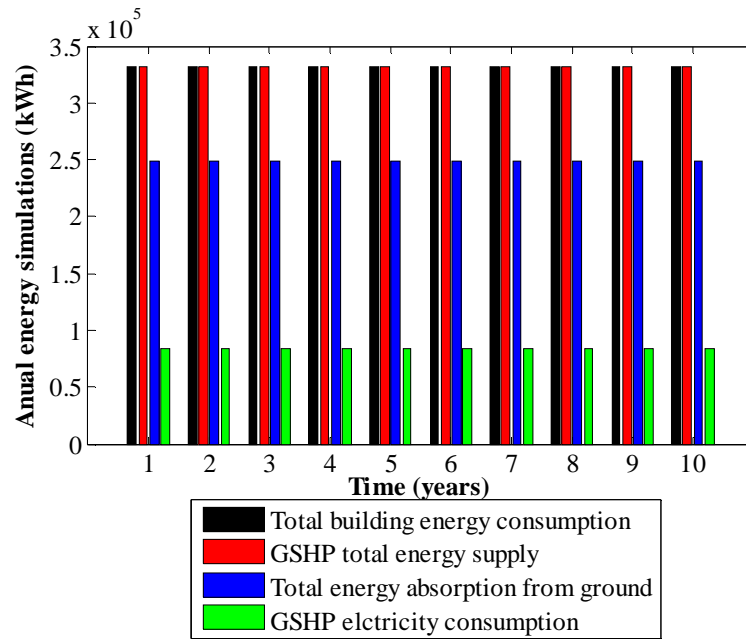
Figure 5-16 Total heating energy consumption of the building and break-down of GSHP energy utilization

Table 5-7 Yearly energy requirement simulations using semi-analytical model

Years	Energy consumption (kWh)	Energy absorbed from ground (kWh)	Energy generated from GSHP (kWh)	Electricity required by GSHP (kWh)
1	332,042	248,343	331,994	83,651
2	332,042	248,332	332,031	83,699
3	332,042	248,325	332,031	83,705
4	332,042	248,322	332,031	83,709
5	332,042	248,320	332,031	83,711
6	332,042	248,318	332,031	83,712
7	332,042	248,317	332,031	83,714
8	332,042	248,316	332,031	83,715
9	332,042	248,315	332,031	83,715
10	332,042	248,315	332,031	83,716

This difference is occurred as economical optimization model neglects hourly variations in the heating energy consumption of the building (it assumes a constant peak load for 12 hours of operations in each heating day for whole 10 year period), heat supplied by GHX over the time and assumes constant heat transfer rates along the borehole wall. This emphasizes the importance in integration of short time step simulations into long time performance of the GSHP systems.

CO_2 emission reduction of the GSHP system against the boiler during the 10 year period is also analyzed. As 2.34 ton of CO_2 is released during the combustion of 1000 liters of diesel and 5.2 ton of CO_2 from the 1TEP (ton of oil equaling to 1.18×10^4 kWh) of electricity production, total CO_2 emission reduction by the GSHP system over the 10 year period is approximately 470 ton. Annual CO_2 emission reduction by GSHP system compared to conventional boiler over 10 year period is illustrated in Figure 5-21. It can be observed that, during the 10 year period, CO_2 emission reduction is decreased slightly. This is due to the thermal depletion of the bore-field over the time.
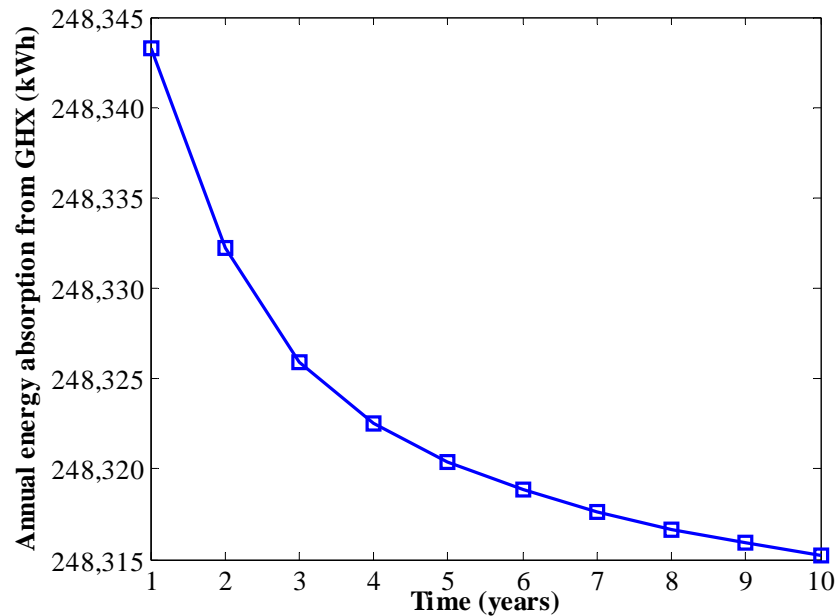
Figure 5-17 variations in the energy absorption from GHX over 10 years
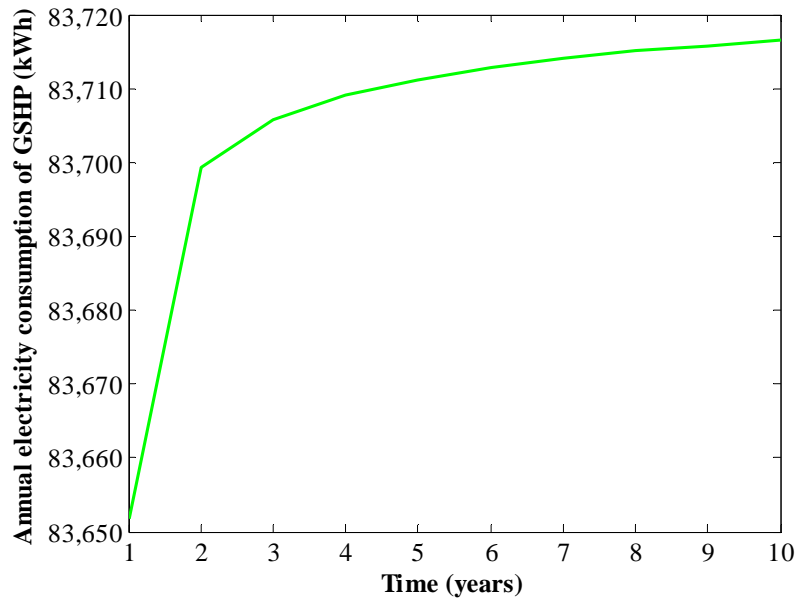
Figure 5-18 variations in electricity consumption of GSHP over 10 years
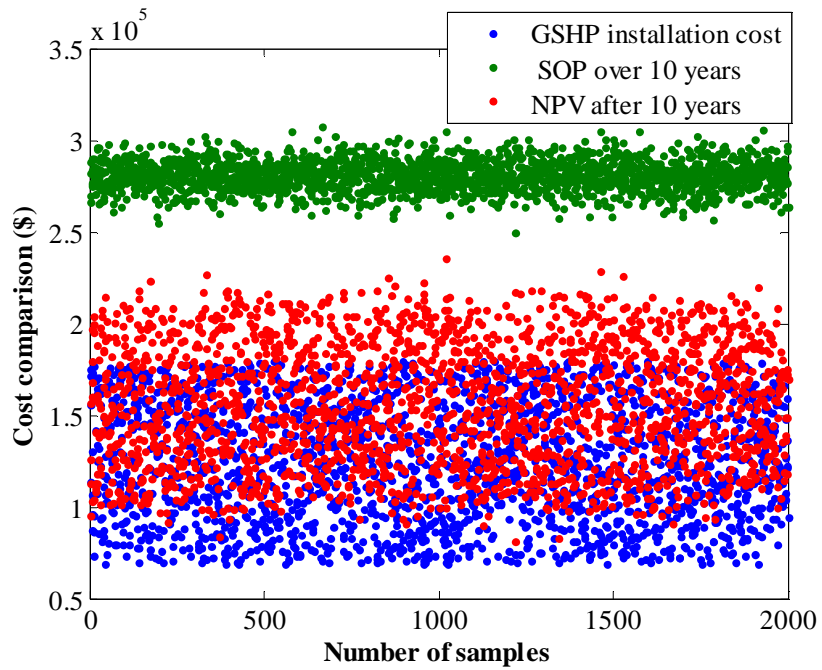
Figure 5-19 Monte-Carlo simulations over 10 year period
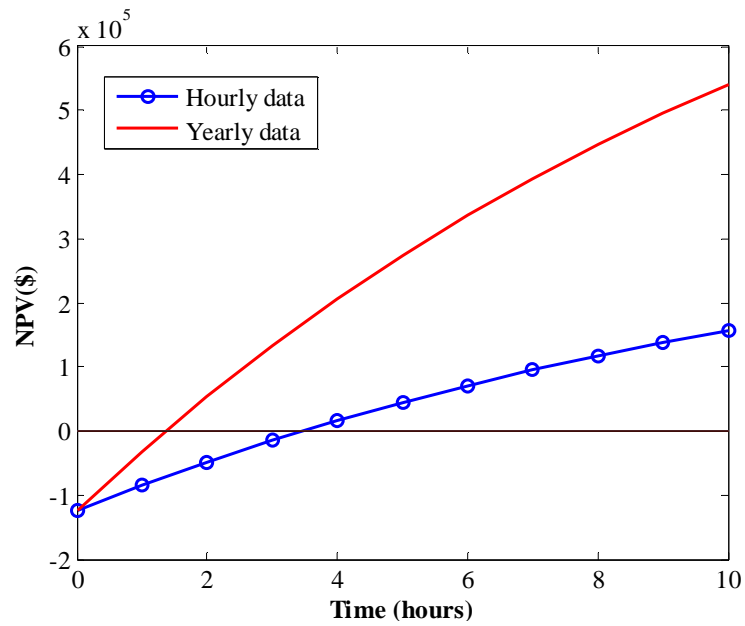
Figure 5-20 Comparison of hourly simulation results and yearly simulation results for break-even point calculations
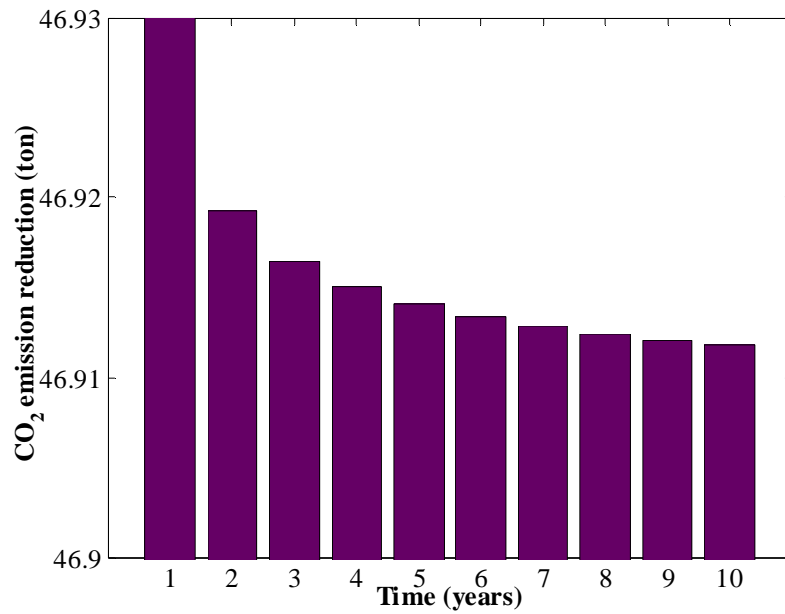
Figure 5-21 CO_2 emission reduction by GSHP compared to conventional boiler

5.6 Summary of the chapter

In this chapter, a numerical methodology for feasibility analysis of GSHP system against a conventional boiler is developed. The model consisted of several sub models, a building load estimation model, GHX design model, economical optimization model and enhanced feasibility analysis. Each model is implemented on a case study at a dormitory building in Middle East technical university, Northern Cyprus campus. The estimated peak hourly heating load of the building is 268,900 W and annual energy consumption is 332,042 kWh. The optimal configuration of the GHX system for a hypothetical GSHP system at dormitory building is a full-sized GSHP system with 28 boreholes (14 x 2) each with 51.47 m long and 3 m apart from each other. Estimated break-even point of GSHP system against the conventional boiler of the dormitory building is 4 years with an assumed annual interest rate of 12%.

CHAPTER 6

CONCLUSION

A new semi-analytical model is developed for analyzing the short term response of the ground heat exchangers by accounting the depth dependencies in the heat transfer rates along the borehole. The model utilizes the solution of Kelvin's infinite-length line source theory to predict the borehole wall temperature. In order to account the variations in the undisturbed ground temperature distribution into line source theory calculations, the computational domain for ground heat exchanger is discretized along its depth. Semi-analytical model results on ground temperature responses for short time steps were compared with literature Yavuzturk and Spitler [3]. They showed a reasonable agreement to each other. Then, semi-analytical model is validated using three dimensional computational fluid dynamics (CFD) simulations developed using OpenFOAM software, which addresses the non-uniform transient behavior of the ground temperature response in sub-hourly intervals at high computational costs. Semi-analytical model results have a good agreement with the CFD model results. The model is capable of evaluating the long term performance of GHX at modest computational costs with intrinsic capabilities of accounting cumulative effects of short-term ground responses without a need to explicitly consider load aggregation.

The developed semi-analytical model is later integrated with the hourly heating loads to analyze the feasibility of GSHP system against a conventional boiler at a dormitory II building in Middle East Technical University Northern Cyprus Campus. The economic feasibility analysis considers the variation in operational cost of the GSHP system due to sub hourly fluctuations in the heating loads, adaptation of fluids' exit and inlet temperatures to GHX in accordance with the hourly demand, uncertainty in the electricity and diesel prices and fuel and electricity price escalations. The effect of thermal degradation on GSHP system is discussed in terms of electricity consumption and the CO_2 emissions over the economic life time.

The economic analysis is consisted of different sub models, a building load estimation model, GHX design model, economical optimization model and enhanced feasibility analysis. Building load estimation model simulates the sub hourly heating loads of the dormitory building using an open source software "OpenStudio" and calculated peak hourly heating load

of the dormitory building as 268,900 W and annual energy consumption as 332,042 kWh. GHX design model estimates the possible design configurations of GHX system for dormitory building. The economical optimization models finds the optimal configuration of GHX for dormitory building as a full-sized GSHP system with 28 boreholes (14 x 2) each with 51.47 m long and 3 m apart. Estimated break-even point against the conventional boiler is 2 years when a constant peak hourly load is assumed to be operated for 12 hours in each heating day over the 10 year period with constant coefficient of performance of 4 for GSHP system. Annual interest rate is assumed as 12% for the NPV calculations. Fuel and electricity price escalations were projected and uncertainty in the cost parameters were accounted using Monte-Carlo simulations.

Finally, enhanced feasibility analysis is carried out for the optimal configuration found in the economical optimization model by integrating the developed semi-analytical model with the hourly heating load data (calculated using OpenStudio software) to study the long term thermal performance of the GSHP system in a monetary sense. It is observed that, heating load demand of a dormitory building during a sample day simulations is mostly matched with the heat pump. However, during the fluids' adaptation periods, the model allows the heat transferred to the space to be over and under the demand curve. Specifically during the times where demand is higher than the supplied heat rate, a backup unit should be used to fully match the demand in this simplified GSHP system.

The break-even point calculations using the hourly performance of the GSHP system is approximately 4 years and it is happened almost 2 years after the one calculate in the optimization model. This demonstrates the importance of studying long term behavior of GSHP system for design and energy analysis with short time steps.

REFERENCES

[1] G. Florides and S. Kalogirou, "Ground heat exchangers—A review of systems, models and applications," *Renew. Energy*, vol. 32, no. 15, pp. 2461–2478, Dec. 2007.

[2] G. Florides and S. Kalogirou, "Annual ground temperature measurements at various depths," in *8th REHVA World Congress, Clima, Lausanne*, 2005.

[3] C. Yavuzturk and J. D. Spitler, "A short time step response factor model for vertical ground loop heat exchangers," *Ashrae Trans.*, vol. 105, no. 2, pp. 475–485, 1999.

[4] Z. Li and M. Zheng, "Development of a numerical model for the simulation of vertical U-tube ground heat exchangers," *Appl. Therm. Eng.*, vol. 29, no. 5–6, pp. 920–924, Apr. 2009.

[5] V. Khalajzadeh, G. Heidarinejad, and J. Srebric, "Parameters optimization of a vertical ground heat exchanger based on response surface methodology," *Energy Build.*, vol. 43, no. 6, pp. 1288–1294, Jun. 2011.

[6] K. Nagano, T. Katsura, and S. Takeda, "Development of a design and performance prediction tool for the ground source heat pump system," *Appl. Therm. Eng.*, vol. 26, no. 14–15, pp. 1578–1592, Oct. 2006.

[7] W. B. Yang, M. H. Shi, and H. Dong, "Numerical simulation of the performance of a solar-earth source heat pump system," *Appl. Therm. Eng.*, vol. 26, no. 17–18, pp. 2367–2376, Dec. 2006.

[8] H. Wang and C. Qi, "Performance study of underground thermal storage in a solar-ground coupled heat pump system for residential buildings," *Energy Build.*, vol. 40, no. 7, pp. 1278–1286, 2008.

[9] J. L. Gaspredes, "Development of an integrated building load-ground source heat pump model as a test bed to assess short- and long-term heat pump and ground loop performance," Dec. 2011.

[10] N. R. C. Government of Canada, "RETScreen International e-Textbook," 11-Aug-2013. [Online]. Available: http://www.retscreen.net/ang/12.php. [Accessed: 11-Aug-2013].

[11] "Geothermal Basics: How Geothermal Energy works, How Heat Pump Works, Types of Ground loops." [Online]. Available: http://www.egshpa.com/renewable-energy/geothermal-basics/geothermal-principle/geothermal-basics/. [Accessed: 25-Jul-2014].

[12] A. D. Chiasson, "Advances in modeling of ground-source heat pump systems," Oklahoma State University, 1999.

[13] A. Mustafa Omer, "Ground-source heat pumps systems and applications," *Renew. Sustain. Energy Rev.*, vol. 12, no. 2, pp. 344–371, Feb. 2008.

[14] L. Jun, Z. Xu, G. Jun, and Y. Jie, "Evaluation of heat exchange rate of GHE in geothermal heat pump systems," *Renew. Energy*, vol. 34, no. 12, pp. 2898–2904, Dec. 2009.

[15] M. Piechowski, "Heat and mass transfer model of a ground heat exchanger: validation and sensitivity analysis," *Int. J. Energy Res.*, vol. 22, no. 11, pp. 965–979, Sep. 1998.

[16] K. Lim, S. Lee, and C. Lee, "An experimental study on the thermal performance of ground heat exchanger," *Exp. Therm. Fluid Sci.*, vol. 31, no. 8, pp. 985–990, Aug. 2007.

[17] J. Busby, M. Lewis, H. Reeves, and R. Lawley, "Initial geological considerations before installing ground source heat pump systems," *Q. J. Eng. Geol. Hydrogeol.*, vol. 42, no. 3, pp. 295–306, 2009.

[18] S. A. Kalogirou and G. A. Florides, "Measurements of Ground Temperature at Various Depths," 2004.

[19] N. Diao, Q. Li, and Z. Fang, "Heat transfer in ground heat exchangers with groundwater advection," *Int. J. Therm. Sci.*, vol. 43, no. 12, pp. 1203–1211, Dec. 2004.

[20] "Ground Temperatures as a Function of Location, Season, and Depth." [Online]. Available: http://www.builditsolar.com/Projects/Cooling/EarthTemperatures.htm. [Accessed: 28-Jun-2014].

[21] H. Zeng, N. Diao, and Z. Fang, "Heat transfer analysis of boreholes in vertical ground heat exchangers," *Int. J. Heat Mass Transf.*, vol. 46, no. 23, pp. 4467–4481, Nov. 2003.

[22] M. A. Bernier, A. Chahla, and P. Pinel, "Long-Term Ground-Temperature Changes in Geo-Exchange Systems," *ASHRAE Trans.*, vol. 114, no. 2, pp. 342–350, Oct. 2008.

[23] C. Yavuzturk, J. D. Spitler, and S. J. Rees, "A transient two-dimensional finite volume model for the simulation of vertical U-tube ground heat exchangers," *ASHRAE Trans.*, vol. 105, no. 2, pp. 465–474, 1999.

[24] M. He, "Numerical modelling of geothermal borehole heat exchanger systems," 2012.

[25] M. Fossa, "The temperature penalty approach to the design of borehole heat exchangers for heat pump applications," *Energy Build.*, vol. 43, no. 6, pp. 1473–1479, Jun. 2011.

[26] W. Thomson, *Mathematical and Physical Papers*. CUP Archive, 2011.

[27] H. S. Carslaw and J. C. Jaeger, *Conduction of Heat in Solids*, 2 edition. Oxford Oxfordshire : New York: Oxford University Press, 1986.

[28] P. Eskilson and J. Claesson, "Simulation Model for Thermally Interacting Heat Extraction Boreholes," *Numer. Heat Transf.*, vol. 13, no. 2, pp. 149–165, 1988.

[29] J. D. Spitler, "GLHEPRO -- A Design Tool For Commercial Building Ground Loop Heat Exchangers," presented at the Proceedings of the Fourth International Heat Pumps in Cold Climates Conference, Aylmer, Québec, 2000.

[30] C. K. Lee and H. N. Lam, "Computer simulation of borehole ground heat exchangers for geothermal heat pump systems," *Renew. Energy*, vol. 33, no. 6, pp. 1286–1296, Jun. 2008.

[31] M. A. Bernier, P. Pinel, R. Labib, and R. Paillot, "A Multiple Load Aggregation Algorithm for Annual Hourly Simulations of GCHP Systems," *HVACampR Res.*, vol. 10, no. 4, pp. 471–487, 2004.

[32] L. Lamarche, "A fast algorithm for the hourly simulations of ground-source heat pumps using arbitrary response factors," *Renew. Energy*, vol. 34, no. 10, pp. 2252–2258, Oct. 2009.

[33] C. K. Lee, "Effects of multiple ground layers on thermal response test analysis and ground-source heat pump simulation," *Appl. Energy*, vol. 88, no. 12, pp. 4405–4410, Dec. 2011.

[34] Y. Nam, R. Ooka, and S. Hwang, "Development of a numerical model to predict heat exchange rates for a ground-source heat pump system," *Energy Build.*, vol. 40, no. 12, pp. 2133–2140, 2008.

[35] R. Fan, Y. Jiang, Y. Yao, and Z. Ma, "Theoretical study on the performance of an integrated ground-source heat pump system in a whole year," *Energy*, vol. 33, no. 11, pp. 1671–1679, Nov. 2008.

[36] M. Z. Olfman, A. D. Woodbury, and J. Bartley, "Effects of depth and material property variations on the ground temperature response to heating by a deep vertical ground heat exchanger in purely conductive media," *Geothermics*, vol. 51, pp. 9–30, Jul. 2014.

[37] K. Charoenvisal, "Energy Performance and Economic Evaluations of the Geothermal Heat Pump System used in the KnowledgeWorks I and II Buildings, Blacksburg, Virginia," Virginia Polytechnic Institute and State University, 2008.

[38] S. Hwang, R. Ooka, and Y. Nam, "Evaluation of estimation method of ground properties for the ground source heat pump system," *Renew. Energy*, vol. 35, no. 9, pp. 2123–2130, Sep. 2010.

[39] A. Siavoshi Kord and S. A. Jazayeri, "Optimization and Analysis of a Vertical Ground-Coupled Heat Pump," *Int. J. Renew. Energy Res. IJRER*, vol. 2, no. 1, pp. 33–37, Mar. 2012.

[40] "How does a heat pump work? - Vent-Axia." [Online]. Available: http://www.vent-axia.com/heatpump/how. [Accessed: 27-Jul-2014].

[41] "Refrigeration: Cop Refrigeration Carnot." [Online]. Available: http://refrigerationbest.blogspot.com.tr/2013/09/cop-refrigeration-carnot.html. [Accessed: 27-Jul-2014].

[42] P. F. Healy and V. I. Ugursal, "Performance and economic feasibility of ground source heat pumps in cold climate," *Int. J. Energy Res.*, vol. 21, no. 10, pp. 857–870, 1997.

[43] G. Gan, S. B. Riffat, and C. S. A. Chong, "A novel rainwater–ground source heat pump – Measurement and simulation," *Appl. Therm. Eng.*, vol. 27, no. 2–3, pp. 430–441, Feb. 2007.

[44] "IITs and IISc elearning Courses in Engineering and Science under NPTEL." [Online]. Available: http://nptel.ac.in/. [Accessed: 20-Jul-2014].

[45] O. M. Al-Rabghi and D. C. Hittle, "Energy simulation in buildings: overview and BLAST example," *Energy Convers. Manag.*, vol. 42, no. 13, pp. 1623–1635, Sep. 2001.

[46] T. Hong, S. K. Chou, and T. Y. Bong, "Building simulation: an overview of developments and information sources," *Build. Environ.*, vol. 35, no. 4, pp. 347–361, May 2000.

[47] D. Garber, R. Choudhary, and K. Soga, "Risk based lifetime costs assessment of a ground source heat pump (GSHP) system design: Methodology and case study," *Build. Environ.*, vol. 60, pp. 66–80, Feb. 2013.

[48] H. Sayyaadi, E. H. Amlashi, and M. Amidpour, "Multi-objective optimization of a vertical ground source heat pump using evolutionary algorithm," *Energy Convers. Manag.*, vol. 50, no. 8, pp. 2035–2046, Aug. 2009.

[49] S. Sanaye and B. Niroomand, "Thermal-economic modeling and optimization of vertical ground-coupled heat pump," *Energy Convers. Manag.*, vol. 50, no. 4, pp. 1136–1147, Apr. 2009.

[50] S. Li, W. Yang, and X. Zhang, "Soil temperature distribution around a U-tube heat exchanger in a multi-function ground source heat pump system," *Appl. Therm. Eng.*, vol. 29, no. 17–18, pp. 3679–3686, Dec. 2009.

[51] P. S. Doherty, S. Al-Huthaili, S. B. Riffat, and N. Abodahab, "Ground source heat pump––description and preliminary results of the Eco House system," *Appl. Therm. Eng.*, vol. 24, no. 17–18, pp. 2627–2641, Dec. 2004.

[52] P. J. Petit and J. P. Meyer, "A techno-economic analytical comparison of the performance of air-source and horizontal-ground-source air-conditioners in South Africa," *Int. J. Energy Res.*, vol. 21, no. 11, pp. 1011–1021, Sep. 1997.

[53] H. Esen, M. Inalli, and M. Esen, "Technoeconomic appraisal of a ground source heat pump system for a heating season in eastern Turkey," *Energy Convers. Manag.*, vol. 47, no. 9–10, pp. 1281–1297, Jun. 2006.

[54] P. Blum, G. Campillo, and T. Kölbel, "Techno-economic and spatial analysis of vertical ground source heat pump systems in Germany," *Energy*, vol. 36, no. 5, pp. 3002–3011, May 2011.

[55] F. P. Incropera and F. P. Incropera, *Fundamentals of heat and mass transfer.* Hoboken, NJ: John Wiley, 2007.

[56] T. Kusuda and P. R. Achenbach, "EARTH TEMPERATURE AND THERMAL DIFFUSIVITY AT SELECTED STATIONS IN THE UNITED STATES," May 1965.

[57] P. Sosnowski and J. Pozorski, "Open-source CFD analysis of multi-domain unsteady heating with natural convection," *TASK Q. Sci. Bull. Acad. Comput. Cent. Gdansk*, vol. 13, pp. 403–414, 2009.

[58] "OpenFOAM® Documentation." [Online]. Available: http://www.openfoam.org/docs/. [Accessed: 18-Jul-2014].

[59] I. Gallego Marcos, "Thermal Mixing CHT Simulations with OpenFOAM: URANS and LES," 2013.

[60] D. Panara and B. Noll, "A coupled solver for the solution of the unsteady conjugate heat transfer problem," *Comput. Methods Coupled Probl. Sci. Eng.*, vol. 2, 2007.

[61] H. Jasak, "Conjugate Simulations and Fluid-Structure Interaction In OpenFOAM." OpenFOAM, Jun-2007.

[62] "Building Technologies Office: EnergyPlus Energy Simulation Software." [Online]. Available: http://apps1.eere.energy.gov/buildings/energyplus/. [Accessed: 20-Jul-2014].

[63] M. Philippe and M. Bernier, "Vertical Geothermal Borefields," *ASHRAE J.*, 2010.

[64] H. S. Carslaw and J. C. Jaeger, *Conduction of heat in solids*. Oxford [Oxfordshire]; New York: Clarendon Press ; Oxford University Press, 1986.

[65] P. Eskilson and J. Claesson, "Simulation Model for Thermally Interacting Heat Extraction Boreholes," *Numer. Heat Transf.*, vol. 13, no. 2, pp. 149–165, 1988.

[66] L. Lamarche, G. Dupré, and S. Kajl, "A new design approach for ground source heat pumps based on hourly load simulations," *month*, vol. 16, pp. 0–02, 2008.

[67] "Brine to Water Heat Pump Water Heater (CGS-95) - China Heat Pump, Brine Water Heat Pump." [Online]. Available: http://sprsun.en.made-in-china.com/product/OKHJlLGUgRWb/China-Brine-to-Water-Heat-Pump-Water-Heater-CGS-95-.html. [Accessed: 28-Mar-2014].

APPENDIX A

CORRELATION COEEFIENTS FOR *F*

Table A-1. The coefficients b_i and c_i for correlation F

i	b_i	c_i
0	7.8189000	*1*
1	-64.2700000	*B/H*
2	153.8700000	$(B/H)^2$
3	-84.8090000	$(B/H)^3$
4	3.4610000	*log(t/ts)*
5	-0.9475300	$log(t/ts)^2$
6	-0.0604160	$Iog(t/ts)^3$
7	1.5631000	*NB*
8	-0.0089416	NB^2
9	0.0000191	NB^3
10	-2.2890000	*A*
11	0.1018700	A^2
12	0.0065690	A^3
13	-40.9180000	$(B/H) \times log(t/t_s)$
14	15.5570000	$(B/H) \times log(t/t_s)^2$
15	-19.1070000	$(B/H) \times NB$
16	0.1052900	$(B/H) \times NB\text{^}2$
17	25.5010000	$(B/H) \times A$
18	-2.1177000	$(B/H) \times A^2$
19	77.5290000	$(B/H)^2 \times log(t/t_s)$
20	-50.4540000	$(B/H)^2 \times log(t/t_s)^2$
21	76.3520000	$(B/H)^2 \times NB$
22	-0.5371900	$(B/H)^2 \times NB^2$
23	-132.0000000	$(B/H)^2 \times A$
24	12.8780000	$(B/H)^2 \times A^2$
25	0.1269700	$log(t/t_s) \times NB$

26	-0.0004028	$log(t/t_s) \times NB^2$
27	-0.0720650	$log(t/t_s) \times A$
28	0.0009518	$log(t/t_s) \times A^2$
29	-0.0241670	$log(t/t_s)^2 \times NB$
30	0.0000968	$log(t/t_s)^2 \times NB^2$
31	0.0283170	$log(t/t_s)^2 \times A$
32	-0.0010905	$log(t/t_s)^2 \times A^2$
33	0.1220700	$NB \times A$
34	-0.0071050	$NB \times A^2$
35	-0.0011129	$NB^2 \times A$
36	-0.0004557	$NB^2 \times A^2$